Magnetic resonance imaging of the wrist, with focus on the triangular fibrocartilage complex and the scapholunate ligament.

Götestrand, Simon

2025

Document Version:
Publisher's PDF, also known as Version of record

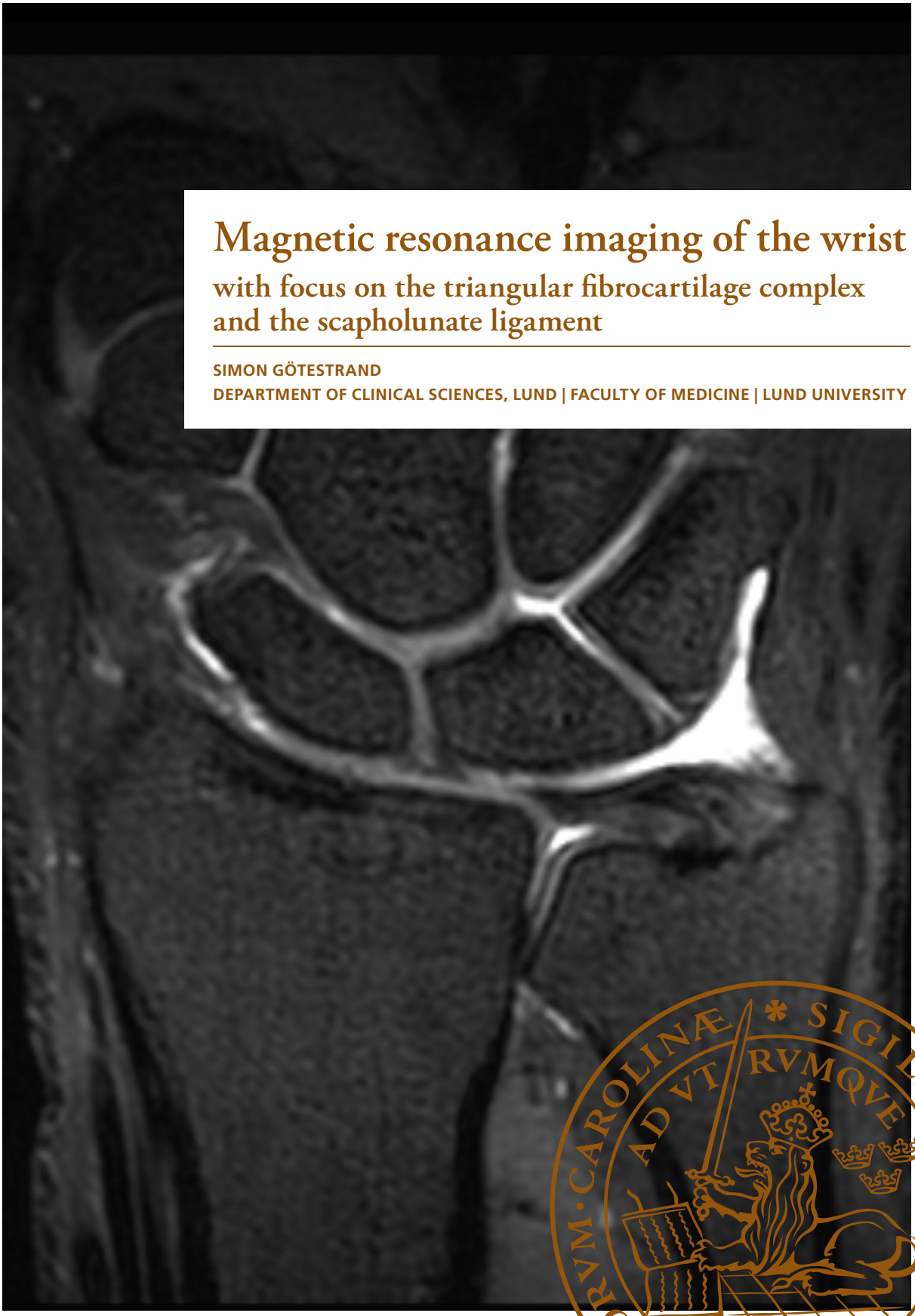

Magnetic resonance imaging of the wrist

with focus on the triangular fibrocartilage complex and the scapholunate ligament

SIMON GÖTESTRAND
DEPARTMENT OF CLINICAL SCIENCES, LUND | FACULTY OF MEDICINE | LUND UNIVERSITY

Magnetic resonance imaging of the wrist

Magnetic resonance imaging of the wrist

with focus on the triangular fibrocartilage complex and the scapholunate ligament

Simon Götestrand M.D.

LUND
UNIVERSITY

DOCTORAL DISSERTATION

Doctoral dissertation for the degree of Doctor of Philosophy (PhD) at the Faculty of Medicine at Lund University to be publicly defended on 26th of September 2025 at 13.00 in föreläsningssal F2, Lund University Hospital, Entrégatan 7

Faculty opponent
Professor Seppo Koskinen, Karolinska Institutet, Stockholm, Sweden

Organization: Lund University, Faculty of Medicine, Department of Clinical Sciences, Diagnostic Radiology

Document name: Doctoral Dissertation **Date of issue:** 2025-09-26

Author: Simon Götestrand

Title and subtitle: Magnetic resonance imaging of the wrist, with focus on the triangular fibrocartilage complex and the scapholunate ligament

Abstract:

Aims: To investigate if visualization of wrist ligaments, and diagnostic accuracy in suspected wrist ligament injury, can be improved with magnetic resonance imaging (MRI) by using a 3D sequence at 3T or by using an ultra-high magnetic field (7T). Further, to investigate the potential role of MRI in the follow-up after scapholunate complex reconstruction.

Methods: In paper I, visualization of wrist ligaments was compared between a 3D sequence and clinical routine 2D sequences, by examining the right wrist of 18 healthy volunteers using 3T MRI. In paper II, visualization of wrist ligaments was compared between 7T and 3T MRI, by examining the right wrist of 18 healthy volunteers at 3T and 7T. In paper III, the symptomatic wrist of 24 patients with suspected wrist ligament injury was examined at 3T and 7T MRI, prior to wrist arthroscopy, to compare the diagnostic accuracy between 7T and 3T MRI in suspected ligament injury, using wrist arthroscopy as a reference standard. In paper IV, to assess the utility of 3T MRI for evaluating long-term graft integrity after scapholunate complex reconstruction, the operated wrist of 13 patients was examined at 3T MRI, 4-13 years after surgery. In paper I-III, the MRI examinations were evaluated and graded individually by four muskuloskeletal radiologists. In paper IV, the MRI examinations were evaluated in consensus by two senior radiologists.

Results: In paper I, visualization of the SLL and the LTL, and portions of the TFCC, was improved by using a 3D sequence compared to 2D-sequences. Paper II showed that visualization of wrist ligaments, cartilage, bone, tendons and nerves was improved by using 7T compared to 3T MRI. Paper III found no difference in diagnostic accuracy, in suspected wrist ligament injury, between 7T and 3T MRI, using wrist arthroscopy as a reference standard. In paper IV, 3T MRI revealed that only one of the evaluated 13 scapholunate complex reconstructions was intact at follow-up, despite good functional outcome in most patients.

Conclusions: Despite improvement in visualization of wrist ligaments by using 7T MRI, the diagnostic accuracy for detecting TFCC and SLL injury was similar at 7T and 3T MRI, and some injuries found using wrist arthroscopy were missed. However, MRI was identified as an important complementary diagnostic tool in suspected wrist ligament injury, providing guidance for the surgeon, and sometimes showing pathologies not discoverable by arthroscopy. In the follow-up after reconstruction of the scapholunate complex, MRI provided new and vital information regarding graft intergrity.

Key words: magnetic resonance imaging; wrist injuries; wrist joint; ligaments, articular; arthroscopies

Classification system and/or index terms (if any) Supplementary bibliographical information

Language: English **Number of pages**: 72

ISSN: 1652-8220

ISBN: 978-91-8021-745-3

Recipient's notes Price Security classification

Signature Date 2025-08-11

Magnetic resonance imaging of the wrist

with focus on the triangular fibrocartilage complex and the scapholunate ligament

Simon Götestrand, M.D.

LUND
UNIVERSITY

Coverphoto by Simon Götestrand (my own right wrist at 7T MR)
Quote on page 7 by Simon Götestrand

Faculty of Medicine
Department of Clinical Sciences, Lund University, Sweden.

ISBN 978-91-8021-745-3
ISSN 1652-8220

Printed in Sweden by Media-Tryck, Lund University
Lund 2025

To challenge our dearest held convictions,
and reject those based on bad evidence,
is the true beauty of the scientific process

Table of contents

Thesis at a glance

Project	Aim	Material & Method	Results	Conclusion
Paper I: Visualization of wrist ligaments with 3D and 2D magnetic resonance imaging at 3 Tesla	To evaluate a 3D sequence optimized for wrist ligament visualization compared to clinical routine 2D sequences at 3T MR.	3D and 2D MRI of the wrist was performed on 18 volunteers.	Most of the evaluated ligament components were better visualized using a 3D sequence compared to 2D sequences.	A 3D sequence can replace 2D sequences in the assessment of wrist ligaments at 3T MRI.
Paper II: Visualization of wrist anatomy – a comparison between 7T and 3T MRI	To investigate if anatomically important structures of the wrist are better visualized at 7T compared to 3T MRI.	7T and 3T MRI of the wrist was performed on 18 volunteers.	All evaluated structures were better visualized at 7T than 3T MRI.	In the absence of pathology, MRI at 7T is superior to 3T in visualization of wrist ligaments, cartilage, trabecular bone, nerves and tendons.
Paper III: MRI of wrist ligament trauma was similar at 7T and 3T with arthroscopy as a reference standard	Comparison of MRI at 7T and 3T in suspected ligament injury, with wrist arthroscopy as a reference standard.	Prior to arthroscopy, 7T and 3T MRI of the wrist was performed on 24 patients with suspected wrist ligament injury.	No statistically significant difference was found between MRI at 7T and 3T in the evaluation of suspected wrist ligament injury.	When wrist ligament injury is suspected, MRI at 7T was not superior to MRI at 3T. However, a majority of injuries were found with MRI at both field strenghts. MRI is a valuable complementray tool to wrist arthroscopy.
Paper IV: Graft integrity after scapholunate ligament reconstruction with tenodesis – improved diagnosis using 3D 3T magnetic resonance imaging	To assess the utility of 3T MRI for evaluating long-term graft integrity after SLL reconstruction.	Clinical examination and MRI was performed on 13 patients 4-13 years after surgery.	Only one of the grafts was intact on MRI. A majority of patients showed improvent in function after surgery.	Using MRI in follow-up studies after SLL reconstruction adds valuable information regarding graft integrity.

Populärvetenskaplig sammanfattning

Handleden består av ett stort antal ben, förbundna med ett komplext system av ligament som skapar stabilitet och som möjliggör avancerade rörelser och funktioner. Ligamentskador i handleden är vanliga, och drabbar ofta unga, aktiva personer. Skador på handledens ligament kan få förödande konsekvenser med inskränkt funktion, instabilitet och smärta. Sekundära progredierande degenerativa förändringar kan ytterligare förvärra symptomen. Utöver att skadan påverkar livskvaliteten finns det en markant samhällsekonomisk effekt, då flertalet är beroende av sina handleder i yrkeslivet.

Det finns många olika metoder för att laga eller rekonstruera skadade ledband i handleden. Vissa av dessa metoder använder patientens egna senor som flyttas för att fungera som ligament.

Historiskt har olika metoder använts för att avbilda handleden i syfte att på ett tillförlitligt sätt diagnostisera ligamentskador som kan kräva handkirurgisk behandling. Postoperativ uppföljning efter rekonstruktion av handledsligament baseras vanligen på klinisk undersökning i kombination med konventionell röntgen, medan magnetkameraundersökning sällan ingår i den rutinmässiga utvärderingen.

Hittills har radiologiska tekniker i hög grad bedömts som otillräckliga för att diagnosticera eller utesluta ligamentskador i handleden, och referensstandarden för diagnostik av dessa skador är titthålsoperation. En bildgivande teknik som inte innebär en operation hade varit en stor fördel för patienterna och även för sjukvården då resurserna i sådana fall skulle kunna frigöras till fördel för terapeutiska titthålsoperationer.

I denna avhandlings första två delarbeten undersöktes friska försökspersoner, för bedömning av hur bra man kan se handledsligament med magnetkamera vid fältstyrkorna 7 och 3 Tesla. Det första delarbetet visade att 3D-teknik gör det lättare att se handledsligament vid 3 Tesla. I det andra delarbetet konkluderades att man ser handledsligament, såväl som brosk, ben, senor och nerver bättre vid 7 Tesla jämfört med 3 Tesla. I avhandlingens tredje delarbete undersöktes patienter med misstänkt handledsligamentskada med MR-undersökning vid 7 och 3 Tesla, och fynden jämfördes sedan med vad man såg när man gjorde titthålsoperation. Ingen säker skillnad i diagnostisk säkerhet fanns mellan MR-undersökning vid de båda fältstyrkorna. I avhandlingens fjärde delarbete utfördes uppföljning flera år efter rekonstruktion av det viktigaste handledsligamentet, med klinisk undersökning och MR. MR visade att rekonstruktionen hade gått sönder i nästan alla patienterna, trots generellt gott kliniskt utfall.

List of papers

Paper I

Götestrand S, Björkman A, Björkman-Burtscher IM, Ab-Fawaz R, Kristiansson I, Lundin B, Geijer M. Visualization of wrist ligaments with 3D and 2D magnetic resonance imaging at 3 Tesla. Acta Radiologica 2022; 63:368-375.

Paper II

Götestrand S, Björkman A, Björkman-Burtscher IM, Kristiansson I, Aksyuk E, Szaro P, Markenroth Bloch K, Geijer M. Visualization of wrist anatomy - a comparison between 7T and 3T MRI. European Radiology 2022; 32:1362-1370.

Paper III

Götestrand S, Flondell M, Lundin B, Aksyuk E, Shalhoub RA, Szaro P, Hedström E, Björkman A, Geijer M. MRI of wrist ligament trauma was similar at 7T and 3T with arthroscopy as a reference standard. European Radiology 2025, doi: 10.1007/s00330-025-11656-4. E-publication ahead of print.

Paper IV

Götestrand S*, Zander M*, Hedström E, Geijer M, Björkman A. Graft integrity after scapholunate ligament reconstruction with tenodesis – improved diagnosis using 3D 3T magnetic resonance imaging. Manuscript.

**shared first authorship*

Author´s contribution to the papers

Paper I and II

Planning the study design. Inclusion of test subjects and scheduling of examinations, including the author´s presence at the MR examinations for image quality control. Collection of data and statistical analysis. Interpretation of results. Creation of figures and tables. Drafting and revising of the manuscripts. Responding to reviewers for resubmission. Collaboration with MR physicists during development of MR sequences at 7T and 3T.

Paper III

All aspects of study design, ethical application, data collection, data analysis, statistical analysis, figures and tables, interpretation of the results, preparation of the manuscript, revision of the manuscript and response to reviewers. Collaboration with operation coordinators at the department of hand surgery for patient inclusion. Coordination with patients for scheduling of MR examinations.

Paper IV

Evaluation of MR examinations and data collection. Interpretation of the results, statistical analysis, figures and tables, and preparation and revision of the manuscript in collaboration with another PhD student.

Abbreviations

2D	Two-dimensional
3D	Three-dimensional
AUC	Area under the curve
DASH	Disabilities of arm, shoulder, and hand questionnaire
FS	Fat suppressed
CI	Confidence interval
CT	Computed tomography
LTL	Lunotriquetral ligament
MPR	Multiplanar reformation
MR	Magnetic resonance
MRA	Magnetic resonance arthrography
MRI	Magnetic resonance imaging
NMR	Nuclear magnetic resonance
NPV	Negative predictive value
PD	Proton density
PPV	Positive predictive value
PRWE	Patient-rated wrist evaluation questionnaire
RF	Radiofrequency
ROI	Region-of-interest
SI	Signal intensity
SLL	Scapholunate ligament
SNR	Signal-to-noise ratio
SPACE	Sampling perfection with application optimized contrasts using different flip angle evolution
T	Tesla
TSE	Turbo spin-echo
TFCC	Triangular fibrocartilage complex
VAS	Visual analogue scale
VGC	Visual grading characteristics

Introduction

Background and aim of thesis

The wrist serves as the connection between the forearm and the hand, comprising the distal ends of radius and ulna and the eight carpal bones[1]. These bones are connected by a complex network of ligaments and other soft tissues. The wrist is of central importance for many of our daily activities, and is considered the most complex joint of the human body[2]. This level of complexity and functionality comes with a high risk of injury[3]. According to some studies, wrist injuries accounts for 2.5% of visits to the emergency department[4], and they are even more common in athletes, where wrist and hand injuries constitute up to 25% of all athletic injuries[5].

In wrist trauma, the most common mechanism is a fall on an outstretched hand, forcing the wrist into hyperextension[6]. In the acute setting, diagnostic attention is usually mostly focused on fractures, and a possible concomitant or isolated ligament injury carries a substantial risk of being left unattended. Traumatic wrist ligament injury is usually suspected when pain and/or instability is experienced in the aftermath of wrist trauma[7]. Untreated, a wrist ligament injury can lead to articular degeneration, with development of osteoarthritis and limitation of wrist functionality[8,9]. Clinical assessment of wrist ligaments is difficult due to the complex anatomy of the wrist and the small size of the ligaments[10].

The current reference standard for diagnosing wrist ligament injury is arthroscopy[11,12]. However, it is a technically demanding procedure, and some areas of the wrist are unavailable for inspection using this technique. Furthermore, it is an invasive method which always comes with risk of complications. For wrist arthroscopy, a systematic review found a complication rate of 4.7%[13]. Reported complications include equipment failure, injury to tendons, nerves and arteries[14], as well as the general risk of infection and complications due to anesthesia. Wrist arthroscopy also carries a vastly larger cost than wrist MRI[15]. It should also be noted that diagnostic wrist arthroscopy, in nonspecific wrist pain, has been shown to be of limited diagnostic value[16].

Several imaging techniques are used in the diagnostic work-up when wrist ligament injury is suspected, e.g. radiography, dynamic radiography with video acquisition, conventional arthrography, CT and MRI, and CT arthrography (CTA) and MR arthrography (MRA). Unfortunately, these techniques often fail to yield reliable and comprehensive results, and therefore arthroscopy is still considered the

best diagnostic method[17]. An imaging modality that offers diagnostic accuracy comparable to wrist arthroscopy would hold significant clinical value. Such a tool could limit the use of arthroscopy to therapeutic purposes, thereby reducing the need for diagnostic invasive procedures, conserving operative resources, and potentially lowering healthcare costs.

In follow-up after reconstructive surgery of the scapholunate ligament (SLL), clinical evaluation and radiographs, and not MRI, are commonly used. Despite a good clinical outcome, malalignment of the scaphoid and the lunate is often seen on radiographs[18].

In contrast to larger joints, the application of MRI in the assessment of wrist ligament injuries has been limited, largely due to the wrist's small size and intricate anatomical structures[19]. With the acquisition of an ultra-high field MRI system (7 Tesla (T)) at Lund University Hospital, the idea for this thesis took form. The overall aims were to investigate (1) if using a 3D sequence at 3T could improve the visualization of wrist ligament structures compared to conventional 2D sequences, (2) compare the visualization of anatomical structures in the wrist between 7T and 3T MRI, (3) compare the diagnostic accuracy in suspected injury to the triangular fibrocartilage complex and the scapholunate ligament between 7T and 3T MRI using wrist arthroscopy as a reference standard, and (4) investigate the potential role of MRI in the follow-up of tendon grafts replacing the scapholunate ligament.

Anatomy of the wrist

Figure 1 shows the bones of the wrist - eight carpal bones and the distal ends of radius and ulna. Carpus can be divided into a proximal and a distal row, with the scaphoid, lunate, triquetrum and pisiform in the proximal row, and the trapezium, trapezoid, capitate, and hamate in the distal row. As demonstrated in Figure 1, the bones fit snugly together, which contributes to both stability and mobility.

The wrist is stabilized by a large number of ligaments, and the complex interconnections between them complicate classification and nomenclature[2,20]. Broadly, they can be divided into extrinsic and intrinsic ligaments, where the extrinsic ligaments connect the distal radius and ulna to the carpal bones, and the intrinsic ligaments create connections between carpal bones[1]. No extensor or flexor tendons attach to the carpal bones, but they contribute to stability and mobility. A simplified overview of dorsal and volar wrist ligaments can be seen in Figure 2.

The wrist can be bent forward (flexion), backward (extension), towards the thumb (radial deviation) and toward the little finger (ulnar deviation). In addition, the hand and forearm can be supinated and pronated, a movement that is made possible by the interaction between the proximal and distal radioulnar joints and several ligaments in the elbow, forearm and wrist.

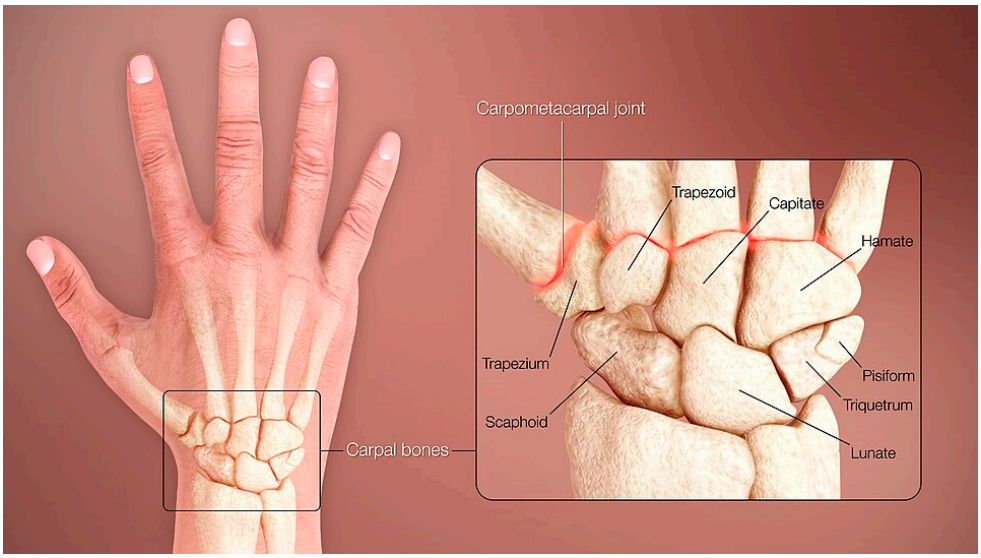

Figure 1. A 3D illustration of the wrist bones. Image credit: Wikimedia Commons. Author: https://www.scientificanimations.com, Creative Commons Attribution-Share Alike 4.0 International license.

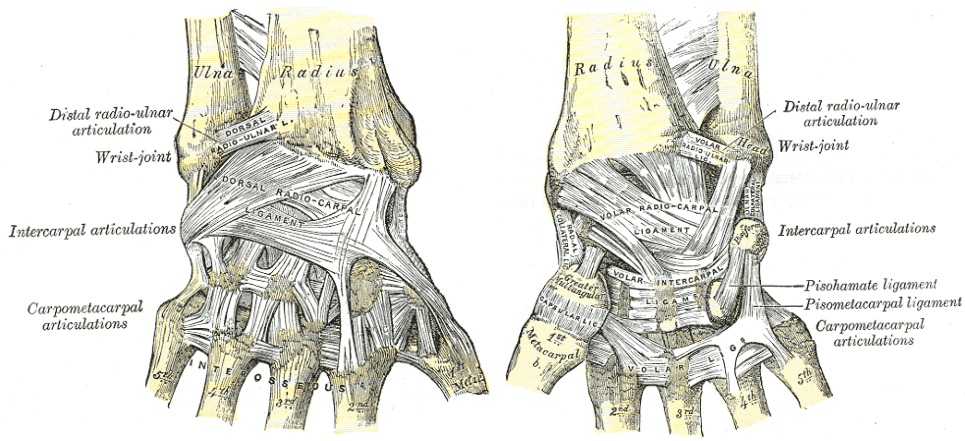

Figure 2. Illustrations of dorsal (left) and volar (right) wrist ligaments. Image credit: Wikimedia Commons. Source: Gray's Anatomy (20th edition). Author: Henry Gray. Illustrator: Henry Vandyke Carter.

The TFCC

The components of the triangular fibrocartilage complex (TFCC) make out the most important stabilizers of the distal radioulnar joint[21]. The distal radioulnar joint together with the proximal radioulnar joint facilitate rotation of the forearm in synchrony with the complex movements of the hand[22]. The anatomical shape of the

distal radioulnar joint makes it intrinsically unstable, necessitating soft tissue stabilizers. The TFCC consist of several interconnected parts[7] (Figure 3 and Figure 4). The dorsal and volar distal radioulnar ligaments connect the distal radius to the ulnar styloid and the ulnar fossa. Between these ligaments is a structure made up of densely packed collagen, called the central articular disk. The ulnolunate and the ulnotriquetral ligaments are also considered part of the complex. They extend between the volar radioulnar ligament and the volar surface of the lunatum and triquetrum, respectively. Finally, the extensor carpi ulnaris tendon and its subsheath and a synovial structure called the ulnomeniscal homologue (not included in Figure 3 or Figure 4), located between the ulnar part of the TFCC and the triquetrum, make up the last parts of the complex.

The SLL and LTL

The intrinsic ligaments connecting the bones of the first carpal row are appropriately named the scapholunate ligament (SLL) and the lunotriquetral ligament (LTL) after the bones they connect. They are sometimes referred to as the scapholunate interosseous ligament (SLIL) and the lunotriquetral interosseous ligament (LTIL). They both have a shape similar to a horse shoe[23,24] (Figure 3), and consist of a dorsal and a volar part, connected proximally by fibrocartilaginous tissue[25]. In the SLL, the dorsal part is the thickest, and biomechanically strongest. On the other hand, the LTL is thicker in and thus stronger in its volar part [24]. A partial tear of either ligament may result in instability[24,26]. A complete tear of the SLL may cause complete carpal collapse[24].

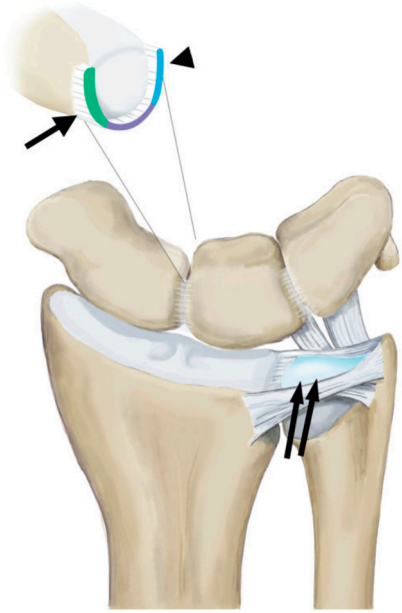

Figure 3. The distal radius and ulna as well as the bones of the proximal carpal row; the scaphoid, lunate and triquetrum. The articular disc (double arrows) is surrounded by the dorsal and volar radiulnar ligaments forming the TFCC. In the top left corner, a sagittal cross-section of the scapholunate ligament is shown, with its thicker dorsal (green; arrow), mostly fibrocartilaginous proximal (purple) and thinner palmar (blue; arrowhead) parts. Artist: Frida Nilsson. Courtesy of Acta Radiologica. 2021, SAGE publications.

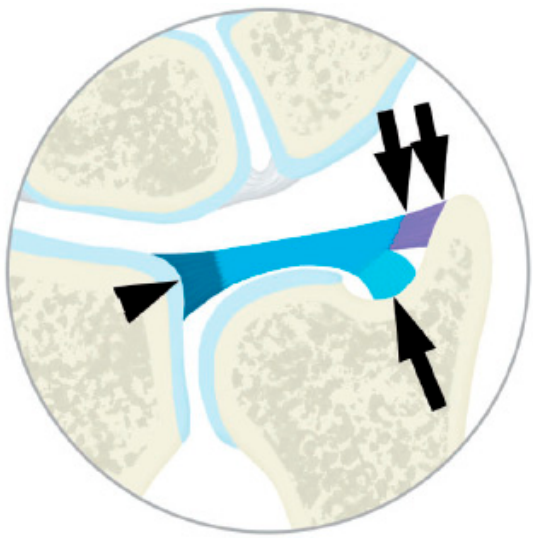

Figure 4. A coronal cross-section of the TFCC, with its radial (dark blue; arrowhead), ulnar styloid (purple; arrows) and ulnar foveal (turquoise; arrow) attachments. Artist: Frida Nilsson. Courtesy of Acta Radiologica. 2021, SAGE publications.

Classification of carpal ligament injury.

The Palmer classification

The most commonly used classification system for TFCC injury is the one developed by Palmer, published in 1989[27]. The classification, which is based on wrist arthroscopy findings, includes both traumatic (type 1) and degenerative (type 2) injuries. Only the classification of traumatic injury will be presented here (Table 1). According to Palmer, a type 1A injury is a central tear of the articular disk. Type 1B is a tear through the radioulnar ligament at its attachment to the ulna. Type 1C is a tear through the ulnolunate and/or ulnotriquetral ligament. Type 1D is a tear though the radioulnar ligament at its attachment to the radius. Notably, the classification does not include tears at the dorsal or volar radioulnar ligaments[28]. Furthermore, it does not differentiate between tears at the foveal and the styloid attachments under type 1B[28,29]. There is also no differentiation between complete and partial tears. Updated or alternative versions of the Palmer classification have been proposed to alleviate these shortcomings[28,30].

Table 1. The Palmer classification of traumatic injury to the TFCC.

Traumatic injury, type:	Description
1A	Central perforation
1B	Ulnar avulsion, with or without concomitant ulnar styloid fracture
1C	Distal avulsion, involving the ulnolunar and/or ulnotriquetral ligaments
1D	Radial avulsion, with or without concomitant radius fracture

TFCC, triangular fibrocartilage complex.

The Geissler classification

For the interosseous ligaments SLL and LTL, the classification developed by Geissler[31] is most commonly applied in arthroscopic practice. The tears are graded as I-IV. The most common serious intercarpal ligament injury is, by far, injury to the SLL. Injuries to the LTL are much less common. The following description is therefore based on a SLL injury. A grade I tear shows no incongruence of carpal alignment, but attenuation or haemorrhage of the ligament is seen from the radiocarpal space. The ligament loses its concave appearance and bulges. In grade II, attenuation or haemorrhage of the ligament can also be seen from the radiocarpal space, but there is additionally an incongruence of carpal alignment, with a slight step-off between the carpal bones when viewed arthroscopically from the mid-

carpal space. Grade III demonstrates a wider gap between the carpal bones, visible from the mid-carpal as well as the radiocarpal space. It is possible to pass through the gap with a small joint probe, but not with a 2.7 mm arthroscope. In grade IV, the gap between the scaphoid and lunate is wide enough to pass through with a 2.7 mm arthroscope.

Comments

The interosseous ligaments may be torn in different ways, which governs how they are repaired. In cases where there are repairable ligament remnants on both sides of the joint, the ligament can be stabilized with a arthroscopic technique according to Mathouline[32]. Some injury types require a combined approach, where the operation partially is done arthroscopically and partially as open surgery. To differentiate between SLL lesions that may benefit from different surgical approaches, Andersson et al. proposed a new classification of dorsal SLL ruptures[32]. Differentiation was made between avulsion of the ligament from the scaphoid (type 1A) and the lunate (type 2A), avulsion fracture from the scaphoid (type 1B) and the lunate (type 2B), rupture through the middle of the ligament (type 3), and partial tear with elongation of the most distal fibres (type 4).

Translating wrist ligament injuries to findings at MRI can be challenging. For example, a TFCC tear at the ulnar styloid is often found to be covered by synovitis at arthroscopy, requiring synovectomy to be visualized[28]. Synovitis result in a signal pattern on MRI that can be difficult to differentiate from an actual tear. If a tear of the SLL is not accompanied by a widening of the scapholunate space, it can be difficult to clearly delineate it using MRI due to its small size.

Wrist arthroscopy

Wrist arthroscopy has its foundations in Japan, where the technologies that underpin modern wrist arthroscopy were developed over a century ago, by Kenji Takagi and Masaki Watanabe[33]. Advancement of the technologies slowly followed, and in the 1980s, they were adapted and translated for safe and standardized use in the wrist joint by Terry Whipple (USA), Gary Poehling (USA) and James Roth (Canada).

In modern wrist arthroscopy, the wrist is placed under traction using a traction device, and a tourniquet is usually utilized for hemostasis[34]. Portals are made to access and evaluate the radiocarpal joint. Apart from inspection, stability tests of the TFCC are performed using an arthroscopic hook and provocation tests. The trampoline test evaluates TFCC compliance, or “bouncing”, by applying pressure with a probe[35]. The hook test evaluates the foveal insertion of the TFCC, which is not visualized through standard portals. It is performed by placing a probe in the prestyloid recess and applying traction radially. The test is positive if the TFCC can

be lifted off the ulnar head[35]. If extensive scar tissue has developed, peripheral TFCC tears may be difficult to diagnose using the hook test. Then, suction can be induced using a shaver. If the test is positive, the suction reveals a loss of tension in the TFCC[36]. This technique can also be utilized to evaluate whether TFCC tension has been restored after repair.

Through the portals, debridement and ligament repair can be performed after diagnosis is made. Peripheral tears of the TFCC are repaired in different ways depending on their severity. Small tears are sutured. Tears associated with distal radioulnar joint instability require TFCC reattachment to the fovea. More advanced lesions require reconstruction with tendon grafts or possibly arthroplasty[30,37]. Radial tears of the TFCC are less common, and it is recommended that non-operative management should be exhausted before repair is considered, which usually can be done using sutures[38].

The SLL can be repaired using sutures if ligament stumps remain attached to the scaphoid and lunate bones[39]. Reconstructive surgery of the SLL is discussed in the next section.

As previously mentioned, diagnostic wrist arthroscopy comes with risk of complications and is costly. New developments in the field may, in part, alleviate these issues. A recent prospective study including 30 patients, using a much smaller instrument; the NanoScope (Arthrex, Naples, FL), showing promising results[15]. Tears of the TFCC, the SLL, the LTL as well as combined tears were diagnosed. No complications were observed, no anesthesia or tourniquet was needed, and the cost of the procedure was much less than conventional diagnostic arthroscopy, but not as low as the cost of wrist MRI. The technique is presented as an alternative to MRI, and the study shows vastly improved sensitivity and specificity compared to MRI. However, the reported sensitivity and specificity for MRI regarding ligament tears, aggregated for TFCC, SLL and LTL tears, was 0.25 and 0.43. This is far lower than the sensitivity and specificity found in most studies previously included in systematic reviews of the subject[17,40], and in paper III of this thesis. The MRI protocol used in the study is not presented, and not all MRI examinations were evaluated by musculoskeletal radiologists. A fairer comparison is warranted between these diagnostic techniques before reliable conclusions can be drawn.

Reconstructive surgery of the SLL

Intercarpal arthrodesis, a traditional treatment for SLL injuries, is associated with loss of wrist motion, altered joint kinematics, and high nonunion rates, often necessitating additional surgery[41]. In the absence of arthritic changes and with reducible carpal malalignment, reconstructive surgery aims to restore scapholunate alignment, alleviate pain, and improve function. Soft-tissue reconstruction has gained popularity due to its potential to preserve better intercarpal kinematics,

although supporting motion data remain limited[42]. Established reconstructive options include capsulodesis[43], tendon graft or bone-ligament-bone autografts[44,45], recreation of a bony or fibrous association between the bones with headless compression screws[46] and limited intercarpal fusion[47]. Among these, tenodesis procedures, which use a tendon graft woven across the scapholunate joint, may offer superior multiplanar control of scaphoid motion compared to capsulodesis[48]. One such technique, the three-ligament tenodesis - a modification of the Brunelli procedure[49] - reconstructs the dorsal SLL while augmenting the scaphotrapeziotrapezoid and dorsal radiocarpal ligaments without tethering to the distal radius[50]. However, reported outcomes of soft-tissue reconstruction vary significantly[42,51].

The fourth paper in this thesis is a follow-up study after scapholunate ligament reconstruction. The reconstructive method used was a tenodesis procedure, as described by Corella et al.[52], using a graft from the flexor carpi radialis tendon. Suitable candidates need to present with 1) a complete tear of the SLL, 2) easily reducible instability and 3) clinical symptoms. The operation pertains five steps. First, bone tunnels are drilled through the scaphoid and the lunate. Second, a suture shaped like a lasso is introduced in the dorsal part of the joint, to prepare for retrieving the graft. Third, an approximately 3 mm wide and 8-10 cm long graft from the radial side of the flexor carpi radialis tendon is cut proximally. Distally, the graft is not severed from the remaining tendon. In the fourth step, the graft is passed from volar to dorsal through the scaphoid bone tunnel created in step 1, using the lasso shaped suture. Following this the graft is passed through the lunate from the dorsal to the volar side. Finally, the end of the graft is passed over the scaphoid joint capsule and radio-scapho-capitate ligament and back to the bore hole in the volar side of the scaphoid. The graft is then fixated using two interference screws, located in the volar end of the scaphoid tunnel and in the dorsal end of the lunate tunnel.

Corella et al. describe satisfactory clinical outcome after the procedure, with improvement in grip strength, reduction of pain and preservation of mobility[52]. Other studies corroborate the finding of reduced pain and improved functionality after reconstruction of the SLL with a tendon graft[50,53].

Imaging methods

Due to its complex anatomy and small size, the wrist is challenging to depict using imaging methods[54]. In evaluation of skeletal trauma, clinical examination is usually complemented with radiographs (X-rays), which often suffice for diagnosis[55]. When a fracture is suspected despite negative findings on radiographs, computed tomography (CT) offers cross-sectional imaging and may reveal occult fractures[56]. In select cases, preoperative CT may be helpful for surgical planning, even when

fractures have already been diagnosed on radiographs[57]. Soft tissues are barely visible with x-ray, and cannot be evaluated in detail with CT, and MR imaging is usually the modality of choice for evaluating soft tissue injuries[58]. In some cases MRI can also be helpful in the diagnosis of fractures[59]. Ultrasound is beneficial in the evaluation of superficial structures, like peripheral nerves, tendons and ganglia, and it has the added advantage of dynamic imaging[58]. However, the incapacity of ultrasound waves to penetrate bone makes evaluation of deeper tissues impossible.

Below follows a brief historical overview of X-ray and CT, including applications in wrist imaging. Thereafter, MRI is described in greater detail, as that is the only imaging modality utilized in the papers included in this thesis.

X-ray

Friday the 8th of November 1895 is considered the birthday of radiology; the day that Wilhelm Conrad Röntgen (Figure 5) noticed a weak fluorescence on a cardboard-screen covered with barium-platinocyanide while experimenting on the absorption by different materials of radiation emitted from an electric gas discharge tube. Further investigations confirmed that a new type of radiation had been discovered, which he named "X-rays"[60]. His findings were published in 1896, and he was awarded the first Nobel Prize for physics in 1901 for the discovery. The first public X-ray image was the left hand of his wife Bertha (Figure 5).

Figure 5. The left hand of Bertha Röntgen; the first public X-ray image (left). Wilhelm Conrad Röntgen (right). Image credit: Deutsches Röntgenmuseum (left) and Wikimedia Commons (right).

Medical application of the new technique was practically instant, with approximately 400 scientific papers on medical aspects of X-rays published in 1896[60]. Since its inception, X-ray has been central in the detection of fractures. However, when wrist ligament injury is suspected, X-ray can only provide indirect signs, such as scapholunate disassociation[61]. In addition, absence of indirect signs does not rule out ligament injury[62]. To better assess carpal ligaments, wrist arthrography was introduced in 1961 by Kesseler and Silberman[63], where contrast medium is injected into different compartments of the wrist joint to detect and characterize ligament tears[64].

Computed tomography (CT)

The invention of CT imaging also resulted in a Nobel Prize, this time awarded to Godfrey Hounsfield (Figure 6) in 1979. He got the brilliant idea of making a three-dimensional depiction of the human body by creating a computer software that combines the information from X-rays passing through the body from multiple different angles[65]. The Nobel Prize was shared with Allan McLeod Cormack, who developed the equations pertaining to CT scanning independently[65].

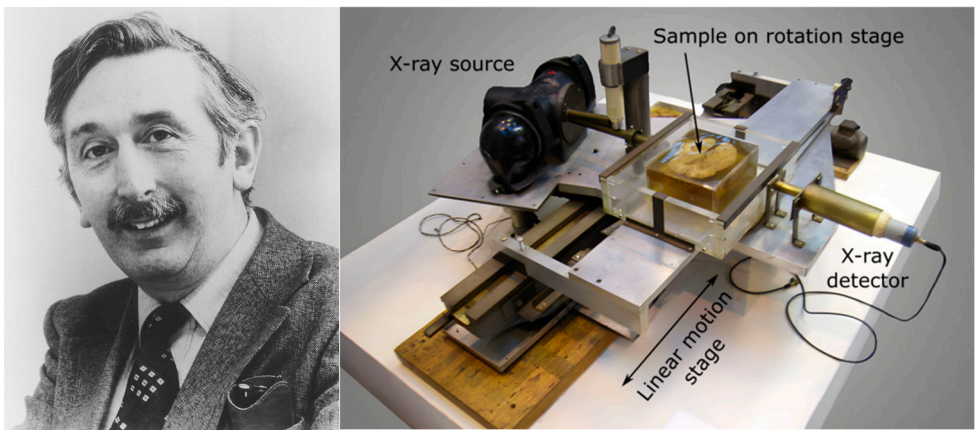

Figure 6. Godfrey Hounsfield (left). The first CT scanner prototype developed by Godfrey Hounsfield in 1968 (right). Image credit: Wikimedia Commons. The right image is based on https://upload.wikimedia.org/wikipedia/commons/3/39/RIMG0277.JPG and was digitally improved and labeled by AlexGustschin, Creative Commons Attribution-Share Alike 4.0 International license.

Evaluation of soft tissues of the wrist, such as ligaments, is limited using CT[62], and similarly to X-ray, CT arthrography was developed to better assess these structures[66,67]. It has been described as an accurate method for detecting tears of the SLL, the LTL, and central tears of the TFCC. However, the accuracy for detecting peripheral tears of the TFCC is lower[68].

Magnetic resonance imaging

The nuclear magnetic resonance (NMR) phenomenon was discovered by Isidor Isaac Rabi in 1938, when he found that molecules emitted radio waves at specific sequences when sent through a magnetic field[69]. He was awarded the Nobel Prize in physics in 1944 for the discovery. The first biomedical study using NMR was published by two Swedish researchers, Erik Odeblad and Gunnar Lindström, in 1955. The characteristics of the NMR signal in calf cartilage was studied using a primitive NMR instrument built by Lindström for his graduate research[70]. Neither Odeblad nor Lindström were awarded a Nobel Prize for their achievements.

Unlike the quick implementation of X-ray in the medical field, it took a long time before the discovery of NMR led to utilization in medical imaging. The first MR scanner built for imaging of the human body was produced in 1977, and a single axial slice through the chest took 4 hours and 45 minutes[69]. In the early 1980s the techniques had been improved, with much shorter acquisition times, and MRI became a part of medical diagnostic imaging[69].

A modern MRI system is usually cubical in shape, with a cylindrical opening in the gantry, and the homogenous volume centred on the central axis. To achieve high signal uniformity and low image distortion, the homogeneity of the basic magnetic field over the examination volume needs to be as high as possible, which is achieved by having this design[71]. The system consists of an outermost superconducting magnet, gradient coils, usually composed of stranded copper strips or copper plates arranged along the inner surface of the magnet, and radiofrequency (RF) coils[72]. The patient table is transferred into the cylindrical lumen in the gantry prior to, and usually stays still throughout, the examination. Figure 7 and Figure 8 show the MR scanners used in study I-III of this thesis.

Figure 7. The 3T MR scanner (Magnetom Vida Fit; Siemens Healthineers) used in study I-III of this thesis. Image credit: Simon Götestrand.

Figure 8. The 7T MR scanner (Achieva 7T; Philips) used in study II-III of this thesis. Image credit: Simon Götestrand.

The magnet generates a uniform magnetic field. The strength of the magnetic field is measured in Tesla (T). In clinical practice, 1.5T and 3T are most used. Magnetic fields of 4T and higher are called ultrahigh magnetic fields[73].

There are three gradient coils built into the scanner. They create electromagnetic fields in three directions perpendicular to each other when electric current flows through them[72,74]. This generates small variations in the uniform magnetic field that are used to create image contrast and to determine where in the sample signal originates.

There are two types of RF coils: a transmit coil and a receiver coil. The transmit coil generates a radiofrequency pulse, creating a small magnetic field perpendicular to the main magnetic field. The strength of this RF pulse determines how much the magnetization is affected in the imaging object (patient). The oscillating magnetic field that thereby emerges from the imaging object results in an induced electric current in the receiver coil. This detected current is the MR signal[72,75]. The MR signal is digitized into data that then is transformed to reconstructed images[76]. Increasing the field strength increases the MR signal. There are many different RF coil designs[77]. In wrist imaging, a coil tailor made for this purpose is essential for maximizing the signal to noise ratio[78]. In the papers included in this thesis dedicated wrist coils were used, developed for 3T and 7T, respectively.

The nuclei of hydrogen atoms are used for clinical MRI due to their abundance in the human body and their strong magnetic moment. The spinning hydrogen nuclei (protons) basically act like miniscule bar magnets, and they interact with the strong and static magnetic field generated by the superconducting magnet. When the transmit coil sends a RF pulse into the body, the spinning nuclei absorb energy and flip out of the equilibrium position. This is called “excitation”. After the RF pulse, the spinning nuclei gradually realign with the longitudinal magnetic field of the superconducting magnet. This is called ”relaxation”, and the energy released during this process causes the electric current in the receiver coil mentioned above. The relaxation rate is different for each tissue type, and the relaxation time of a tissue type is called its T1. Thus, the different MR signals originating from different tissues in a T1-weighted image depend on this relaxation time of the tissues.

Apart from being affected by the longitudinal magnetic field of the MR scanner, the magnetization of the excited spinning nuclei also affect each other, in the transverse plane. The time it takes for equilibrium to be reached between the spinning nuclei in a tissue is called its T2. Thus, in a T2-weighted image, the MR signals originating from different tissues depend on the speed of this relaxation time[79].

The relative T1- and T2-weighting of an image depends on a sequence’s repetition time (TR) and echo time (TE). TR is the time between RF pulses transmitted, and TE is the time until the MR signals are measured in the transverse plane. A long TE result in a high T2-weighting, as the tissues have time to generate a lot of signal from gradual transverse relaxation. A short TR does not allow time for complete longitudinal relaxation before the next RF pulse. Therefore, more

signal is received from tissues with fast T1 relaxation than from tissues with slow T1 relaxation, resulting in T1-weighting of the image. For example, fluid-filled areas of the body, like synovial fluid in joints, have a short T2 and therefore generate a lot of signal in a T2-weighted image. More aqueous tissues generally have longer T1, and therefore lower signal on a T1-weighted image[79].

7T MRI

7T MRI systems have been manufactured for approximately two decades[80]. Thus far, they have mostly been used for research, but since the first approval for clinical use for neurological and musculoskeletal applications was given in 2017[81], this will probably become more common. Advantages of using an ultrahigh magnetic field are improved signal gain and a shortened scan time, or increased spatial resolution[81], or a compromise between these advantages. Increasing the field strength increases the MR signal, making 7T very beneficial for high spatial resolution imaging, which inherently has a low signal.

Some of the challenges of using an ultrahigh magnetic field are that RF interference effects, such as central brightening, are more pronounced[73,82], and that the higher radiofrequency energy transmitted causes a higher degree of tissue heating[80]. These challenges are less pronounced in wrist imaging than in imaging of most other parts of the body, as RF interference effects are limited by the small size of the wrist[83], and RF energy deposition is less marked in the extremities than in the head and trunk[80]. Another challenge is that T1 increases at higher field strengths, resulting in longer scan times in T1-weighted imaging[84].

The gantry in a 7T MRI system is narrower than at lower field strengths, which may cause discomfort to some patients. Dizziness, inconsistent movement, nausea, metallic taste and headache are short term, subjectively experienced side effects frequently reported from test subjects and patients after 7T MRI examinations[85]. However, these side effects have been shown to decrease over time when subjected to repeated examinations at 7T[85].

Magnetic resonance arthrography (MRA)

Just like with X-ray and CT, arthrography was developed for MRI. It can be minimally invasive, with a contrast medium administered intravenously (indirect MRA), or more invasive, with contrast medium injected into the radiocarpal joint, (direct MRA)[86]. Direct MRA has the advantage of fully distending the joint space, with contrast outlining ligament tears and passing through defects[87]. Both direct and indirect MRA have previously been shown to be superior to MRI in detecting wrist ligament injuries[12,40,88,89]. Henceforth, direct MRA will be referred to just as MRA, as this is the technique meant when using the term. Using diagnostic arthroscopy as a reference standard, a recent study found MRA to have a sensitivity of 0.81, a

specificity of 1.0 and an accuracy of 0.96 in detecting peripheral TFCC lesions[87]. The study did not include enough SLL lesions for statistical analysis regarding this structure. Regarding the SLL, a recent paper was published with the purpose of establishing evidence-based consensus statements on imaging of scapholunate joint instability by an expert group consisting of 27 musculoskeletal radiologists[90]. Among the statements, MRA was deemed superior to MRI in providing diagnostic accuracy in the assessment of SLL tears, and MRA (along with CTA) was stated as the imaging methods providing the most accurate diagnosis of SLL lesions, supplemented by dynamic studies, if essential[90]. To further improve the visualization of wrist ligament tears, axial traction during MRA has shown promising results[91]. This technique also improves the visualization of articular cartilage.

Magnetic resonance arthrography was not evaluated in the papers included in this thesis. The purpose was to evaluate completely non-invasive MR methods, i.e. using 3D-sequences and an increased field strength.

Developing MRI sequences

Developing a 3D sequence at 3T

The protocol used for 3T MR, in paper I-III of this thesis, was the standard clinical wrist protocol at Lund University Hospital, with the addition of a 3D sequence developed by MR physicists Jimmy Lätt and Peter Mannfolk. This 3D sequence was used as a template and an inspiration for creating a 3D sequence at Sahlgrenska University Hospital that, in addition to the local clinical wrist protocol, was used for paper IV of this thesis. During the development of the 3D sequence, the images were continuously evaluated using a diagnostic radiological perspective, with adjustments and fine tuning until images of satisfactory quality were achieved. The main priority was, apart from generally high image quality, optimal delineation of ligaments. To increase the signal-to-noise ratio (SNR), and thus achieving sharper images, the field of view was increased to include a part of the forearm and most of the hand (220x150 mm). This allows for a higher number of phase encoding steps, which leads to a higher SNR. The downside is a longer scan time, which increases the risk of motion artefacts. A maximal sequence duration of approximately seven minutes was decided upon, to balance the gains from an increased SNR against the risk of artefacts. As participant fatigue, and thereby the risk of motion artefacts increases with scan duration, the 3D sequence was acquired first as it had the longest acquisition time. The total wrist MR protocol should also have a reasonably short acquisition time for feasible clinical application.

Different 3D sequences have previously been used and recommended for visualization of wrist ligaments[54,92–96]. We chose a proton density (PD) weighted turbo spin-echo (TSE) sequence with special modifications optimizing it for isotropic 3D imaging. PD-weighted sequences are suitable for ligament imaging[97].

As the name implies, tissues with a high density of protons give rise to the highest signal in PD-weighted imaging. This is achieved by minimizing both T1-weighting and T2-weighting, by having a long TR and a short TE. Ligaments, which contain very little hydrogen, are seen as markedly black on this sequence. Spin echo sequences have historically not been used in 3D imaging due to their unacceptably long acquisition times and / or associated artefacts. However, through different design strategies and optimization, acquisition times and artefacts have been reduced[98]. The name of the optimized 3D sequence depends on the manufacturer. The MRI system used at our 3T system is made by Siemens, and their name for the sequence is SPACE. The acronym "SPACE" stands for "Sampling Perfection with Application optimized Contrasts using different flip angle Evolution". The Philips version of the sequence is called "Volume Isotropic Turbo spin echo Acquisition", with the catchy acronym "VISTA", and General Electric calls their equivalent sequence "CUBE" which is just a name, and not a creative acronym.

Developing sequences at 7T

When developing MR sequences at 7T, we had to start from scratch. Using the wrist sequences at 3T as a template and inspiration, MR physicist Karin Markenroth built the sequences, receiving immediate and continuous feedback from a radiologist's perspective. The initial work took a long time, with reliance on colleagues (including ourselves) and other volunteers as test subjects. However, most participants did not want to lay in the crammed and claustrophobic gantry of the system for more than 30 minutes at a time. Because of the slow progress, the approach was changed. Local butchers were contacted, and eventually one who would contribute with the hind leg of a pig was found – naturally in the name of scientific progress. The pork cut was placed in a plastic bag containing water, and thus the perfect candidate for initial sequence optimization was in place. For the final stretch, application specialist Fredy Visser in Utrecht was contacted, and he joined in for a couple of days of fine tuning of the sequences. During this stage of the optimization work, human volunteers were used yet again.

Previous findings

3D MRI of the wrist

3D imaging is increasingly utilized in musculoskeletal MR imaging. It can achieve thinner contiguous slices than 2D sequences, provide improved spatial resolution and allows for multiplanar reconstruction (MPR)[99]. It can also reduce scan time, as one 3D sequence potentially can replace three 2D sequences in the coronal, axial and sagittal plane.

In a study including 69 patients with wrist pain, Park et al. found similar image quality between a 3D sequence and 2D sequences in the depiction of the TFCC[100]. Rehnitz et al. concluded that a 3D sequence provided the highest image quality regarding the TFCC and wrist ligaments in a study comparing different 2D and 3D sequences, including 18 patients with wrist pain and 16 healthy volunteers[54]. A 3D sequence was found superior to 2D sequences in imaging of the SLL in a study including 10 healthy volunteers by Jung et al.[101].

MRI vs wrist arthroscopy

In recent years, two systematic reviews have been carried out to evaluate the usefulness of MRI in in the evaluation of wrist ligament tears[17,40]. Great variation was found, but generally, diagnostic accuracy of MRI was found to be inferior to wrist arthroscopy. The results from the studies included in the two systematic reviews, published in 2015 and 2020 respectively, are summarized in Table 2. A more detailed review of the findings is presented below.

The systematic review by Andersson et al. in 201517 found that negative results of MRI cannot safely rule out clinically relevant tears to the TFCC or the SLL and the LTL, and concluded that arthroscopy remains the preferred diagnostic technique when it comes to wrist ligament injuries. A wide range of predictive values was found in the included studies (PPV 71-100% and NPV 37-90% for the TFCC, PPV 25-100% and NPV 72-94% for the SLL, PPV 0-100% and NPV 74-95% for the LTL). Only seven studies were included in the review, where six studies investigated the TFCC, three investigated the SLL, two investigated the LTL and one evaluated the performance of diagnosing partial SLL and LTL injuries. Kato et al.[102] found the sensitivity, specificity and accuracy of finding TFCC tears using 3D versus 2D MRI as 1.0, 0.53 and 0.79 versus 0.83, 0.67 and 0.76. In the study by De Smet et al.[103], the sensitivity and specificity of MRI in suspected TFCC tears were 0.61 and 0.88. Manton et al.[104] investigated the sensitivity and specificity of MRI in finding partial tears of the SLL and the LTL. The findings were reported separately for two observers, with a sensitivity of 0.69 and 0.42 and a specificity of 0.32 and 0.81 for the SLL. For the LTL, the sensitivity was 0.36 and 0.25 and the specificity was 0.68 and 0.84. Magee[105] found the sensitivity of MRI in suspected tears of the TFCC, SLL and LTL as 0.86, 0.89 and 0.82. The specificity was 1.0 for all three structures. In suspected TFCC tear, Blazar et al.[106] reported their findings separately for two observers, with the sensitivity, specificity and accuracy of MRI as 0.86 vs 0.80, 0.96 vs 0.80, and 0.83 vs 0.61. Lastly, Morley[107] found the lowest precision of MRI in diagnostics of TFCC and SLL tears, with a sensitivity of 0.44 and 0.11, and specificity of 0.87 and 0.30.

In 2020, Krastman et al. conducted a systematic review that included 16 studies evaluating injuries to wrist ligaments[40]. The TFCC and the SLL was investigated in 12 studies and the LTL was investigated in eight studies. However, using arthroscopy as the reference test and MRI as the index test, only five studies

included an investigation of the TFCC[11,89,108–110], four studies of the SLL[89,108,109,111] and three studies of the LTL[89,108,109]. The study conducted by Anderson et al. included 102 patients presenting with ulnar-sided wrist pain[108]. It was retrospective and found improvement of sensitivity, specificity and accuracy in suspected injury of the TFCC, SLL and LTL at 3T compared to 1.5T MRI, but not matching those of arthroscopy. Boer et al. could not confirm the superiority of MRI at 3T compared to 1.5T in their retrospective study, including 150 patients presenting with wrist pain, and arthroscopy was again found superior[110]. Note that only the TFCC was evaluated in this study. Prosser et al. found MRI findings of TFCC, SLL and LTL injuries "moderately useful", "mildly useful" and "not useful" respectively in their retrospective study of 105 patients presenting with wrist pain[109]. Pahwa et al. carried out a prospective study including 16 patients with MRI performed prior to arthroscopy[89]. The sensitivity of detecting tears of the TFCC, SLL and LTL with MRI was 83.3%, 63% and 40% respectively. The study by Schmauss et al. included a much larger number of patients (908), but the study was retrospective and limited to suspected TFCC injury only[11]. The sensitivity and specificity for detection of arthroscopically verified TFCC lesions was 76% and 41% respectively. Finally, the sensitivity and specificity for SLL tears with MRI was 79% and 82% respectively in the retrospective study by Greditzer et al., including 26 patients[111].

Table 2. The sensitivity and specificity of MRI in suspected wrist ligament injury, using arthroscopy as a reference standard, found in previous studies, as reported in two systematic reviews. * The results are from two independent observers. † The results are from observations using coronal and axial sequences respectively.

Author (year)	Field Strength	Structure	Sensitivity (%)	Specificity (%)
Kato et al. (2000)	1.5T (3D)	TFCC	100	53
	1.5T (2D)	TFCC	83	67
Manton et al. (2001)	1.5T	SLL	42 / 69*	32 / 81*
	1.5T	LTL	25 / 36*	68 / 84*
Blazar et al. (2001)	Not specified	TFCC	80 / 86*	80 / 96*
Morley (2001)	1.5T	TFCC	44	87
	1.5T	SLL	11	30
De Smet et al. (2005)	Not specified	TFCC	61	88
Anderson et al. (2008)	1.5T	TFCC	82	69
	3T	TFCC	90	74
	1.5T	SLL	57	83
	3T	SLL	70	94
	1.5T	LTL	22	94
	3T	LTL	50	94
Magee (2009)	3T	TFCC	86	100
	3T	SLL	89	100
	3T	LTL	82	100
Pahwa et al. (2014)	1.5T	TFCC	83	100
	1.5T	SLL	63	100
	1.5T	LTL	40	100
Schmauss et al. (2016)	Not specified	TFCC	76	41
Greditzer et al. (2016)	1.5T	SLL	65 / 79†	69 / 82†
Boer et al. (2018)	1.5T	TFCC	71	75
	3T	TFCC	73	67

LTL, lunotriquetral ligament; SLL, scapholunate ligament; T, Tesla; TFCC, triangular fibrocartilage complex.

Follow-up MRI after ligament reconstruction

Long-term follow-up studies using MRI to evaluate the status of grafts replacing the SLL after reconstructive surgery have not been published prior to this thesis. However, multiple follow-up studies using MRI have been published regarding grafts replacing the anterior cruciate ligament of the knee[112].

Worldwide, anterior cruciate ligament reconstruction is one of the most commonly performed orthopedic procedures[113]. The autograft is usually taken from the patella or hamstring tendon. In a systematic review of studies evaluating biopsies from anterior cruciate ligament reconstructions histologically, the graft is described as going through a "ligamentization" process, where it gradually goes through changes and eventually resembles a native anterior cruciate ligament[114]. The stages are simplified into an early-, remodelling- and a maturation stage. This maturation can roughly be visualized and evaluated using MRI, as the graft gradually loses signal as it matures, due to decreased water content[115,116]. Apart from a visual assessment, MRI evaluation is done by placing regions of interest (ROIs) in the graft, wherein the mean signal intensity (SI) is measured[115–121], and a signal ratio using the posterior cruciate ligament as reference is usually obtained.

The SLL is much smaller than the anterior cruciate ligament, and it is uncertain if SLL grafts are big enough to place ROIs in them to obtain reliable SI measurements. This was attempted in the fourth paper of this thesis, as part of the assessment of long-term graft integrity. Apart from directly evaluating the reconstruction grafts, graft integrity was assessed by measuring the scapholunate distance, the scapholunate angle, evaluating the bore canals though the scaphoid and the lunate and assessment of degenerative changes. Potential osteolysis around the screws fixating the tendon graft to the scaphoid and the lunate was also evaluated. All patients included in the fourth study of this thesis had received bioabsorbable interference screws, and osteolysis has previously been described as more common around bioabsorbable screws than around nonabsorbable interference screws[122].

Radiography is the reference standard for measurements of the scapholunate angle. Measurements using MRI may potentially be misleading, as a perfectly neutral position of the wrist during the examination cannot be expected. However, no difference between radiographs, MR and CT was found in a study comparing measurements of the scapholunate angle between the three modalities[123]. The authors explain this by asserting that the position of the wrist does not affect the positional relationship between the scaphoid and the lunate.

Aims

To investigate if visualization of wrist ligaments, and diagnostic accuracy in suspected wrist ligament injury, can be improved with MRI by using a 3D sequence and an ultra-high magnetic field (7T). Further, to investigate the potential role of MRI in the follow-up after scapholunate complex reconstruction.

Paper I

The aim was to evaluate a 3D sequence optimized for wrist ligament visualization compared to clinical routine 2D sequences at 3T MR.

Paper II

The aim was to investigate if visualization of important structures of the wrist, most importantly ligaments, could be improved by using ultra-high field MR (i.e. 7T) compared to 3T MR.

Paper III

The aims were to investigate *1)* if the diagnostic accuracy is higher for 7T MRI than 3T MRI in suspected wrist ligament injury; and *2)* if wrist ligament injury can be ruled out with MRI at 7T or 3T using wrist arthroscopy as a reference standard.

Paper IV

The aim was to assess the utility of 3T MRI for evaluating long-term graft integrity after reconstruction of the scapholunate ligament.

Material & methods

Study population

The studies were carried out in accordance with the declaration of Helsinki. The Regional Ethical Review board in Lund, Sweden, approved studies I-III (2017/193). The Swedish ethics review authority (Etiksprövningsmyndigheten) approved study IV (2021-01114 and 2024-02747-01). Written informed consent was acquired from all participants prior to participation.

For studies I and II, 18 healthy subjects were included in each study. The groups consisted of nine female and nine male participants between 20 and 49 years of age, with three female and three male subjects from each decade. Seven of the subjects participated in both studies. In those cases, new MR examinations were performed for the second study, and no images from study I were reused in study II. The right wrist was always chosen for examination. Inclusion criterion for both studies was a clinical hand and wrist examination without pathological findings, carried out by an expert[124] hand surgeon. Exclusion criteria were subjective symptoms from the right wrist that could indicate pathology, contraindications to MRI or not being able to understand spoken or written instructions in Swedish.

In study III, 24 patients (18 years or older) were included. Inclusion criteria were suspected wrist ligament injury by an expert hand surgeon and a scheduled wrist arthroscopy. Exclusion criteria were contraindications to MRI or not being able to understand spoken or written instructions in Swedish. Every patient that was found suitable was contacted and asked if they wanted to participate.

In study IV, 13 patients who had received a SLL reconstruction 4-13 years before were included. The age at the time of the MRI examination ranged between 30-62 years. The inclusion criterion was receiving a SLL reconstruction at least four years prior to the follow-up. Exclusion criteria were contraindications to MRI or revision surgery after the primary surgery.

Recruiting participants

For the first two papers, the recruitment was not difficult. It turned out to be easy to find 18 healthy test subjects willing to participate amongst colleagues at the department of radiology. A clinical examination conducted by an expert hand surgeon ascertained that no signs of wrist injury were present. The 7T and 3T MRI scanners could be booked for a couple of days, and all examinations could be conducted in a few batches.

The third paper proved vastly more difficult. The study participants should be patients with wrist pain, and suspicion of TFCC and/or SLL injury should be raised by a hand surgeon. A wrist arthroscopy should also be scheduled. The start of the recruitment process coincided with the COVID-19 pandemic, which reduced the number of elective wrist arthroscopies to near zero; wrist pain can be debilitating, but diagnosis and treatment of ligament injury can usually wait. After the pandemic, the waiting list for elective hand surgery was long, and a shortage of operating nurses further delayed these operations. However, a close collaboration with the operation coordinators at the department of hand surgery was established, and contact was made every time arthroscopy was planned for a patient who could be a potential participant. After making sure the inclusion criteria were fulfilled, the patients were contacted and asked if they would like to participate in the study. Most patients obliged, for which I am grateful. Thus began the quest to find examination slots at both the 7T and 3T MRI scanners on the same day, before the arthroscopy date. This was taxing, but almost always possible, thanks to the helpful staff at both MR scanners and the MRI booking coordinators.

For the fourth study, 25 out of 44 patients participating in a follow-up study investigating the clinical outcome after arthroscopic SLL reconstruction, conducted at the department of hand surgery, Sahlgrenska University Hospital in Gothenburg, were invited to participate in the study. Inclusion was done by a hand surgeon, and 13 patients accepted. Clinical examination was performed by a senior hand surgeon, who also sent the referral for the MRI.

MRI protocols

In the first study, the 3T protocol included a 3D PD-weighted SPACE sequence acquired in the coronal plane, 2D PD-weighted sequences acquired in three orthogonal planes, with fat saturation in the coronal and sagittal, but not in the axial plane, and a T1-weighted sequence acquired in the coronal plane. The acquisition time for the 3D sequence was 7 minutes 5 seconds, and the total acquisition time for all sequences was 23 minutes 33 seconds.

In the second and third study, the 3T protocol was the same as for the first study, except that fat saturation was utilized for the 2D PD-weighted sequences in all

planes. Similarly to the 3T protocol, the 7T protocol consisted of a 3D PD TSE sequence acquired in the coronal plane, 2D PD-weighted sequences with fat saturation acquired in three orthogonal planes, and a T1-weighted sequence acquired in the coronal plane. The acquisition time for the 3D sequence was 7 minutes 7 seconds, and the total acquisition time for all sequences was 20 minutes 18 seconds.

In the fourth study, the 3T protocol included a 3D PD-weighted SPAIR sequence, a PD-weighted SPAIR TSE sequence and a T1-weighted TSE sequence, all acquired in the coronal plane, a PD-weighted Dixon TSE sequence acquired in the axial plane, and a PD-weighted TSE sequence acquired in the sagittal plane. The total acquisition time was 16 minutes, 9 seconds.

Typical parameters for the three 3D sequences are presented in Table 3.

Table 3. Typical parameters for the 3D sequences.

	3D PD SPACE	3D PD SPAIR	3D PD TSE
Paper	I – III	IV	II - III
Field strength	3T	3T	7T
Repetition time (ms)	1.100	1.200	1.100
Echo time (ms)	39	115	110
Echo train length (ms)	29	19	22
Reconstructed voxel dimensions (mm^3)	0.5x0.5x0.5	0.4x0.4x0.4	0.24x0.24x0.24
Aquisition time (min:sec)	7:05	4:48	7:07

3D, three-dimensional; PD, proton density; SPACE, sampling perfection with application optimized contrasts using different flip angle evolution; SPAIR, spectral attenuated inversion recovery; TSE, turobo spin-echo.

Number and choice of observers in radiology studies

In paper I, II and III of this thesis, four musculoskeletal radiologists with various degrees of experience in musculoskeletal MRI and wrist diagnostics evaluated the images separately. The same four radiologists were not used in the different studies. Imaging studies should have multiple observers[125]; it is vital for reliable and generalizable findings, especially when the evaluated structure or structures are known to be difficult to assess. The results of paper III signify this.

In the 12 studies included in two different systematic reviews mentioned previously[17,40], none had a number of observers exceeding three. Two of the studies[11,110] used findings of clinical MRI examinations as their data, and not new observations. Three of the studies only had one observer[103,107,109], and it appears that the observer in one of the studies was not a radiologist but a hand surgeon[107]. Four studies had two observers[104–106,108] and three studies had three observers[89,102,111]. In

one of these studies[102], the three observers were hand surgeons, described as having experience in assessing MR images. In 2023, a study by Heiss et al. was published comparing image quality of 7T and 3T wrist MRI in 25 participants with chronic wrist pain, with a control group consisting of 25 participants with no wrist pain[126]. Unusually, and impressively, seven observers were used, all of whom were musculoskeletal radiologists.

The number of observers should be chosen based on the goals of the study and should routinely be more than one[125]. For generalizable results, several observers are essential, and the experience should vary between the observers. The choice of observers is also important – of the above-mentioned studies, the one with lowest specificity of TFCC and SLL tears at MRI was a study with a hand surgeon as the sole observer[107]. Contrarily, if the sole observer were the leading expert in the field globally, the findings would most likely not be applicable to a realistic, clinical setting.

VGC analyzer statistical software

The statistical software Visual grading characteristics (VGC) analyzer[127,128] was used to analyse data in the first three papers of this thesis. As this statistical method is tailored for visual grading by multiple observers, but not commonly used, it deserves a special mention and explanation.

In visual grading, the numbers obtained do not have a real numerical value, and the span between the numbers is not fixed. Hence, these values must not be treated as numbers mathematically or statistically. For the data to be correctly analysed, this mandates a non-parametric, rank invariant method. In VGC analysis, the ratings for two conditions are compared by producing a VGC curve. The curve is a plot of the proportion of ratings above a threshold for a reference condition, against the same proportion for a test condition. For example, the reference condition could be the visualization of a ligament with MRI at 3T, and the test condition could be the visualization of the same ligament with MRI at 7T. One observer might score the reference condition as 2 and the test condition as 3, while another observer scored the conditions as 3 (reference) and 4 (test). In a standard statistical analysis, this would mean complete disagreement. However, with ordinal data, their change in assessment is the same: one step higher score for the test condition.

The area under the curve is the measure of separation between the two conditions. The value of the AUC is always between 0 and 1. If the AUC is above 0.5, the test condition is better than the reference condition. If the AUC is exactly 0.5, there is no measurable difference between the two conditions. If the AUC is lower than 0.5, the reference condition is superior to the test condition. To determine the standard deviation and a confidence interval, a bootstrapping resampling technique is used. In statistical bootstrapping, a single data set is resampled to create numerous

simulated samples[129]. To determine a *p*-value, a permutation resampling technique is used, where the proportion of times a test statistic exceeds a permuted null distribution is computed to test the null-hypothesis[130]. An example of a VGC curve can be seen in Figure 9.

The receiver operating characteristic (ROC) analysis creates a curve similar to that of the VGC analysis. However, unlike the VGC analysis, the ROC analysis assumes independence between the two conditions it compares, which is not applicable in visual grading of the same structures, using different sequences or field strengths.

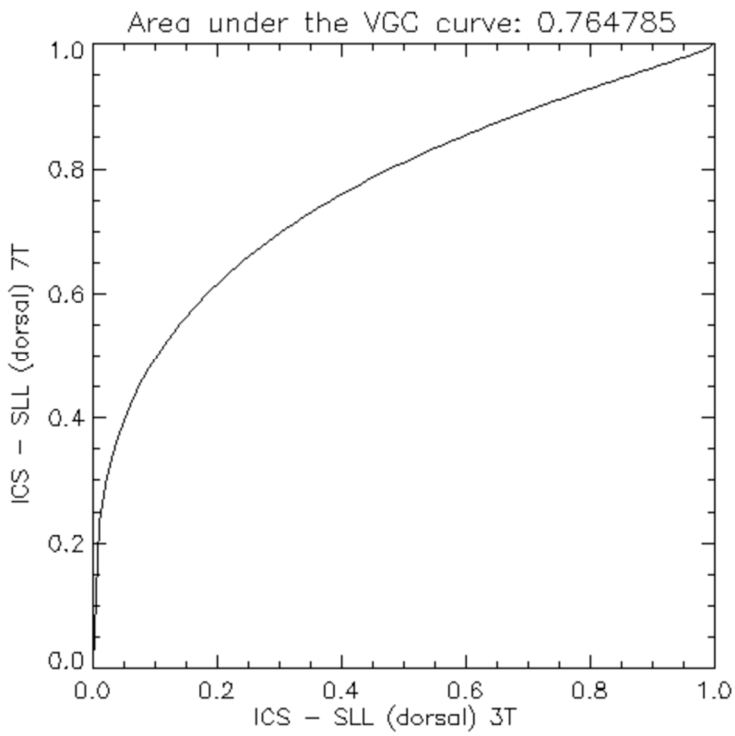

Figure 9. An example of a VGC curve
The VGC curve based on the visual grading of the dorsal part of the SLL at 7T compared to 3T. The AUC is 0.76 - well over 0.5, with a confidence interval 0.66 – 0.85 (*p*-value <0.0001). This means that the dorsal part of the SLL was better visualized at 7T compared to 3T, and the finding is statistically significant. *AUC, area under the curve; SLL, scapholunate ligament; VGC, visual grading characteristic.*

Evaluating functional outcome

In the fourth paper of this thesis, long-term functional outcome after reconstructive wrist ligament surgery was assessed by using two validated questionnaires, the disability of the arm, shoulder and hand (DASH) and the patient-rated wrist evaluation (PRWE) questionnaires. Both questionnaires were in Swedish and have been validated in Sweden. The scores were compared with scores collected prior to surgery. In the DASH questionnaire, the patient reports disability and symptoms by attributing scores between 1-5 on a Likert scale, with a total of 30 questions[131]. Similarly, in the PRWE questionnaire, the patient reports difficulty in performing various wrist functions and presence of pain by attributing scores between 0-10 on a Likert scale, with a total of 15 questions[132]. In both questionnaires, a high score indicates a high level of disability.

Results and Discussion

The following section is a summary of the findings with comments for each study. A detailed description of the results from each study can be found in the actual papers; part II of this thesis.

Paper I

In this study, visualization of separate components of the TFCC, the SLL and the LTL was compared between a new 3D sequence, that had been optimized for wrist ligament visualization, and the clinical routine wrist MRI protocol. Eighteen healthy test subjects were included. The clinical routine protocol consisted of four 2D sequences. Image evaluation was done individually by four musculoskeletal radiologists, and the VGC Analyzer was used for statistical analysis.

Visualization of the dorsal and volar portions of the SLL and the LTL was improved using a 3D sequence compared to 2D sequences. For the TFCC, there was only a statistically significant difference in visualization of the foveal attachment, with the 3D sequence being superior. Image quality was measured using three parameters – edge sharpness, perceived tissue contrast and presence of artifacts. No statistically significant difference was found between 3D and 2D imaging using either of these parameters. Please note that Bonferroni correction for multiple comparisons was used, and $P < 0.005$ was considered as statistically significant.
The results of the VGC analysis are shown in Table 4. MR images showing comparison between visualization of the SLL using 3D and 2D are shown in Figure 10.

Table 4. Visual grading characteristic analysis, comparing ratings between 3D and 2D imaging.
An AUC_{VGC} of 0.5 indicates that the image quality on average is rated equally for the 3D sequence and the 2D sequences. An AUC_{VGC} of >0.5 indicates that the image quality of the 3D sequence is superior. An AUC_{VGC} of <0.5 indicates that the image quality of the 2D sequence is superior. If there is a statistically significant difference between ratings, the confidence interval does not contain 0.5. *P* values in bold typeface indicate significant changes after Bonferroni correction.

VGC analysis	AUC_{VGC} (95% CI)	*P* value
TFCC, radial attachment	0.62 (0.39-0.83)	0.096
TFCC, ulnar styloid attachment	0.69 (0.51-0.83)	0.011
TFCC, foveal attachment	0.69 (0.53-0.84)	**0.002**
SLL dorsal portion	0.78 (0.64-0.91)	**0.001**
SLL palmar portion	0.82 (0.68-0.94)	**<0.001**
LTL dorsal portion	0.93 (0.81-1.0)	**<0.001**
LTL palmar portion	0.89 (0.75-0.98)	**<0.000001**
Edge sharpness (image quality)	0.34 (0.17-0.52)	0.019
Perceived tissue contrast (image quality)	0.58 (0.29-0.87)	0.15
Artifacts (image quality)	0.65 (0.54-0.75)	0.018

AUC, area under the curve; CI, confidence interval; LTL, lunotriquetral ligament; SLL, scapholunate ligament; TFCC, triangular fibrocartilage complex; VGC, visual grading characteristic.

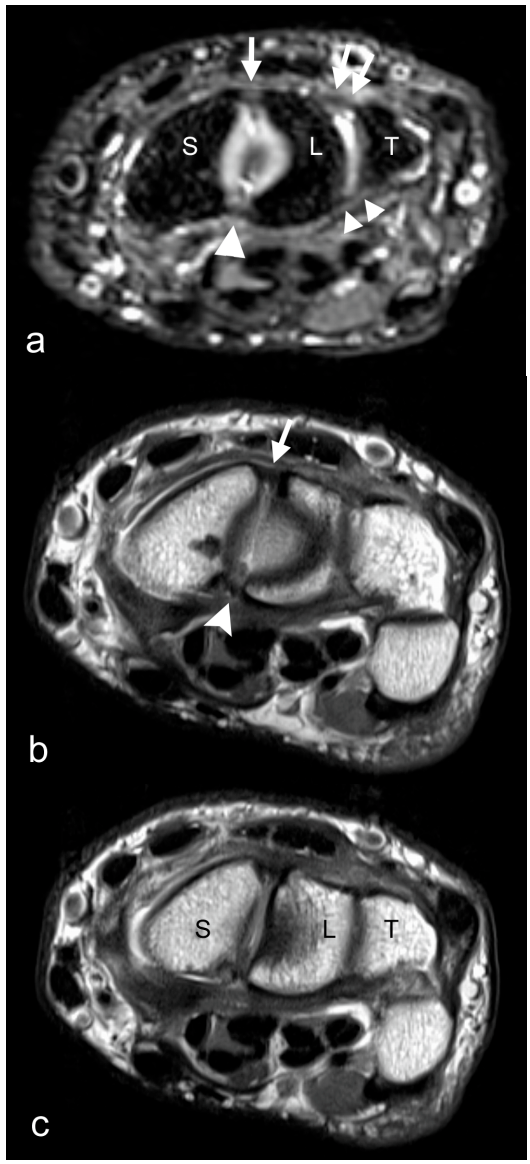

Figure 10. Depiction of the SLL and LTL on 3D and 2D imaging. (a) A 0.5-mm thick axial section from a 3D SPACE sequence, manually reformatted to allow visualization of the dorsal (arrow) and palmar (arrowhead) part of the SLL as well as of the dorsal (arrows) and palmar (arrowheads) part of the LTL. (b, c) A 2-mm thick axial 2D PD sequence offers visualization of the dorsal part of the SLL (arrow in b). The palmar part of the SLL is shown sub-optimally (arrowhead in b), and the dorsal and palmar part of the LTL are not well seen due to suboptimal alignment of the structures and the lack of ability to perform MPR in a plane optimized for visualization of the ligaments. *2D, two-dimensional; 3D, three-dimensional; L, lunate; LTL, lunotriquetral ligament; MPR, multiplanar reformations; PD, proton density; S, scaphoid; SLL, scapholunate ligament; SPACE, sampling perfection with application optimized contrasts using different flip angle evolution; T, triquetrum.* Courtesy of Acta Radiologica. 2021, SAGE publications.

The benefits of 3D imaging for visualization of the small, intrinsic SLL and LTL was the most cogent finding. This is where the advantage of multiplanar reformation of thin slices is most evident. It has previously been found that the SLL is best viewed on axial sequences[111], but with 3D imaging, the radiologist does not have to limit image evaluation to one plane. The finding that 3D imaging is advantageous in imaging of the SLL corroborates the findings by Jung et al.[101].

The superiority of 3D imaging regarding the TFCC was not as apparent as for the SLL and LTL in this study, where improved visualization was only evident in one of the evaluated parts of the complex. Whether visualization of the TFCC benefits from 3D imaging remains uncertain, as it was previously found beneficial by Park et al.[100], but not by Jung et al.[101].

In summary, all evaluated structures were equally or better visualized using a 3D sequence compared to 2D sequences. Thus, a 3D sequence can replace 2D sequences when wrist ligaments need to be assessed.

Paper II

In this study, visualization of ligaments, bone, cartilage, tendons and nerves, in 18 healthy test subjects, was compared between 7T and 3T MRI. Image evaluation was done individually by four musculoskeletal radiologists, and the VGC Analyzer was used for statistical analysis.

Visualization of all evaluated structures was improved with MRI at 7T compared to 3T. Imaging with a 3D sequence and 2D sequences were graded separately, and 7T was superior to 3T for all structures in both instances. Please note that comparison between 3D and 2D imaging was not done in this study.

Imaging at 7T also resulted in better image quality than 3T regarding edge sharpness and perceived tissue contrast. No significant difference was found regarding artefacts. The results of the VGC analysis are shown in Table 5 and Figure 11. Examples with comparison between 7T and 3T MRI of different structures are shown in Figure 12 and 13.

Table 5. VGC analysis, comparing ratings between 7T and 3T MR.

An AUC_{VGC} of 0.5 indicates that the image quality on average is graded equally at 7T and 3T MR. An AUC_{VGC} of >0.5 shows that the image quality is superior at 7T. An AUC_{VGC} of <0.5 shows that the image quality is superior at 3T. If there is a statistically significant difference between grading, the confidence interval does not contain 0.5.

VGC analysis	AUC_{VGC} (95% CI)	*P* value
TFCC, radial attachment (3D)	0.70 (0.61-0.78)	<0.0000001
TFCC, radial attachment (2D)	0.62 (0.53-0.71)	0.011
TFCC, ulnar styloid attachment (3D)	0.74 (0.67-0.81)	<0.0000001
TFCC, ulnar styloid attachment (2D)	0.68 (0.60-0.76)	<0.0000001
TFCC, foveal attachment (3D)	0.75 (0.69-0.81)	<0.0000001
TFCC, foveal attachment (2D)	0.67 (0.58-0.76)	0.0025
SLL dorsal portion (3D)	0.73 (0.68-0.78)	<0.0000001
SLL dorsal portion (2D)	0.76 (0.66-0.85)	<0.0000001
SLL palmar portion (3D)	0.65 (0.56-0.72)	0.0075
SLL palmar portion (2D)	0.72 (0.62-0.81)	0.0025
LTL dorsal portion (3D)	0.66 (0.60-0.72)	0.0005
LTL dorsal portion (2D)	0.71 (0.61-0.81)	0.0005
LTL palmar portion (3D)	0.65 (0.55-0.74)	0.022
LTL palmar portion (2D)	0.65 (0.59-0.72)	0.001
Trabeculae of the capitate bone	0.87 (0.81-0.91)	<0.0000001
Cartilage (triquetrum/hamatum) (3D)	0.84 (0.79-0.88)	<0.0000001
Cartilage (triquetrum/hamatum) (2D)	0.73 (0.65-0.81)	<0.0000001
Tendon (ECU) (3D)	0.73 (0.63-0.83)	0.0005
Tendon (ECU) (2D)	0.78 (0.67-0.87)	<0.0000001
Median nerve (3D)	0.80 (0.72-0.87)	<0.0000001
Median nerve (2D)	0.82 (0.72-0.91)	<0.0000001
Ulnar nerve (3D)	0.80 (0.72-0.86)	<0.0000001
Ulnar nerve (2D)	0.88 (0.78-0.94)	<0.0000001
Edge sharpness (image quality)	0.74 (0.68-0.80)	<0.0000001
Percieved tissue contrast (image quality)	0.73 (0.67-0.78)	<0.0000001
Artifacts (image quality)	0.52 (0.42-0.60)	0.714

AUC, area under the curve; CI, confidence interval; ECU, extensor carpi ulnaris; LTL, lunotriquetral ligament; SLL, scapholunate ligament; TFCC, triangular fibrocartilage complex; VGC, visual grading characteristic.

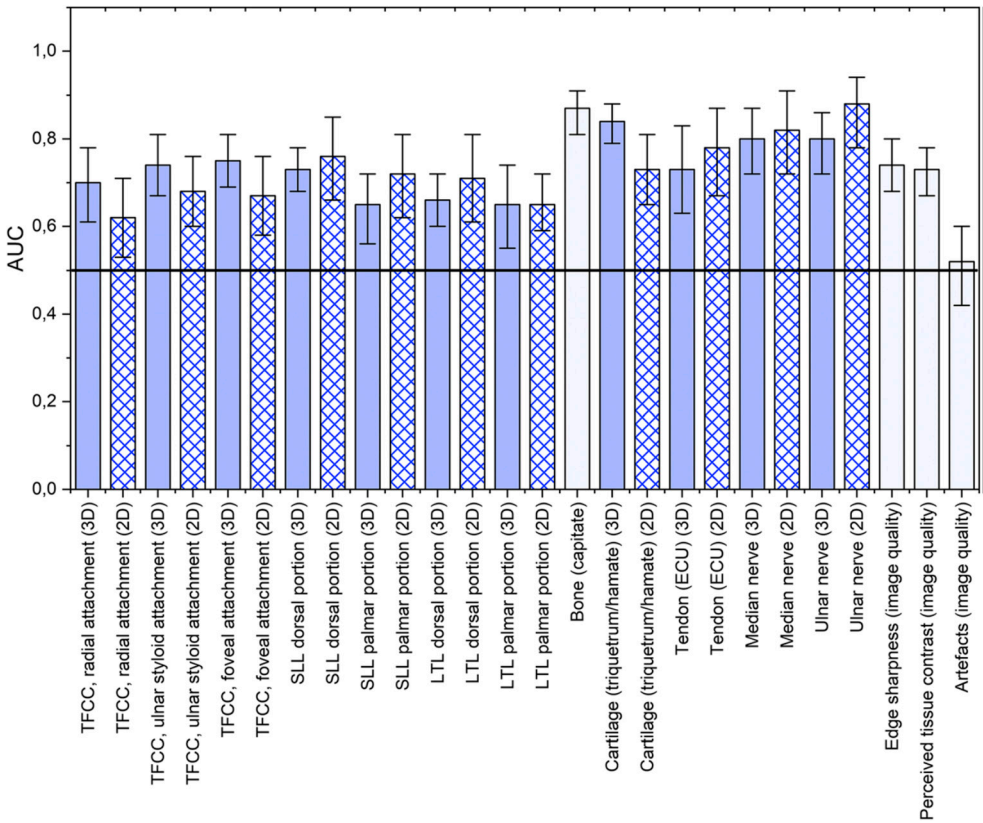

Figure 11. VGC analysis comparing grading between 7T and 3T imaging. If the bar showing the AUC, including the range bar representing the confidence interval, is above 0.5, 7T imaging was on average graded significantly better than 3T imaging. Wider confidence intervals imply lower observer agreement. *AUC, area under the curve; ECU, extensor carpi ulnaris; LTL, lunotriquetral ligament; SLL, scapholunate ligament; TFCC, triangular fibrocartilage complex; VGC, visual grading characteristic.* Courtesy of European Radiology. 2021, Springer Nature. License CC BY 4.0

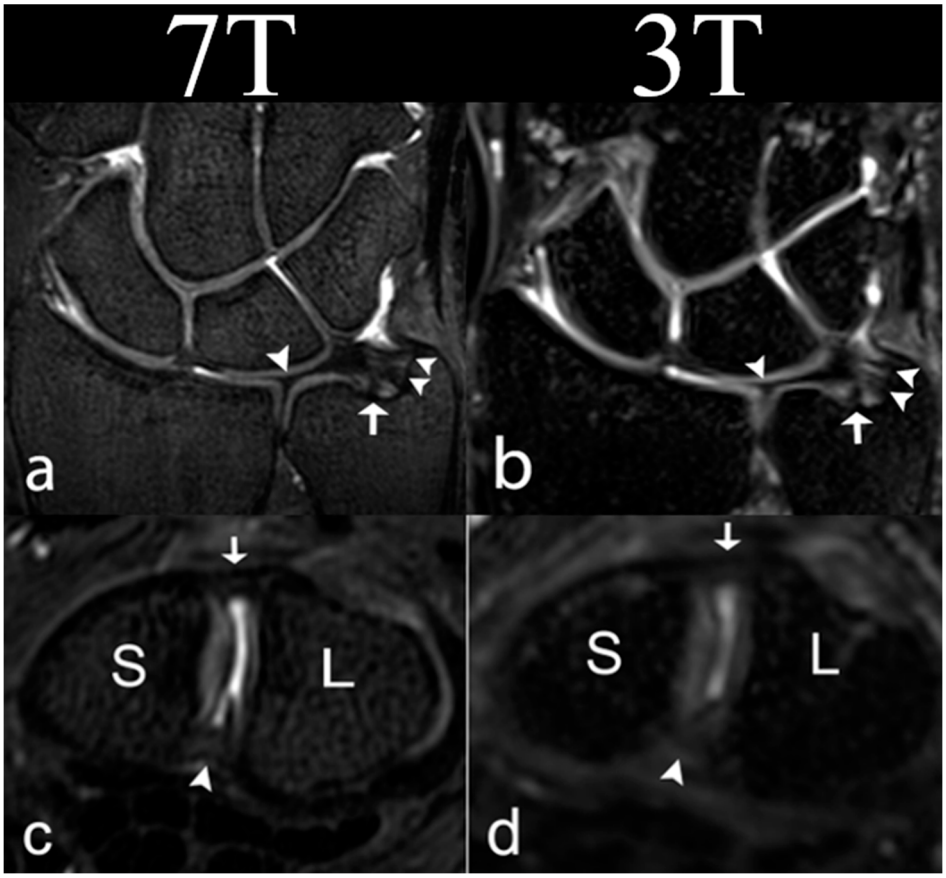

Figure 12. A 32-year-old male healthy volunteer (a, b), a 22-year-old male healthy volunteer (c, d). **a** A 7T 0.5-mm-thick coronal 3D PD TSE section and (**b**) a 3T 0.5-mm-thick coronal 3D PD SPACE section with a depiction of the ulnar styloid attachments (arrowheads), the foveal attachment (arrow) and the radial attachment (arrowhead) of the TFCC. **c** A 7T 0.5-mm-thick axial 3D PD TSE section and (**d**) a 3T 0.5-mm-thick axial 3D PD SPACE section with visualization of the dorsal portion (arrow), and the palmar portion (arrowhead) of the SLL. *L, lunate; PD, proton density; S, scaphoid; SLL, scapholunate ligament; SPACE, "sampling perfection with application-optimized contrasts using different flip angle evolution"; TFCC, triangular fibrocartilage complex; TSE, turbo spin echo*. Courtesy of European Radiology. 2021, Springer Nature. License CC BY 4.0

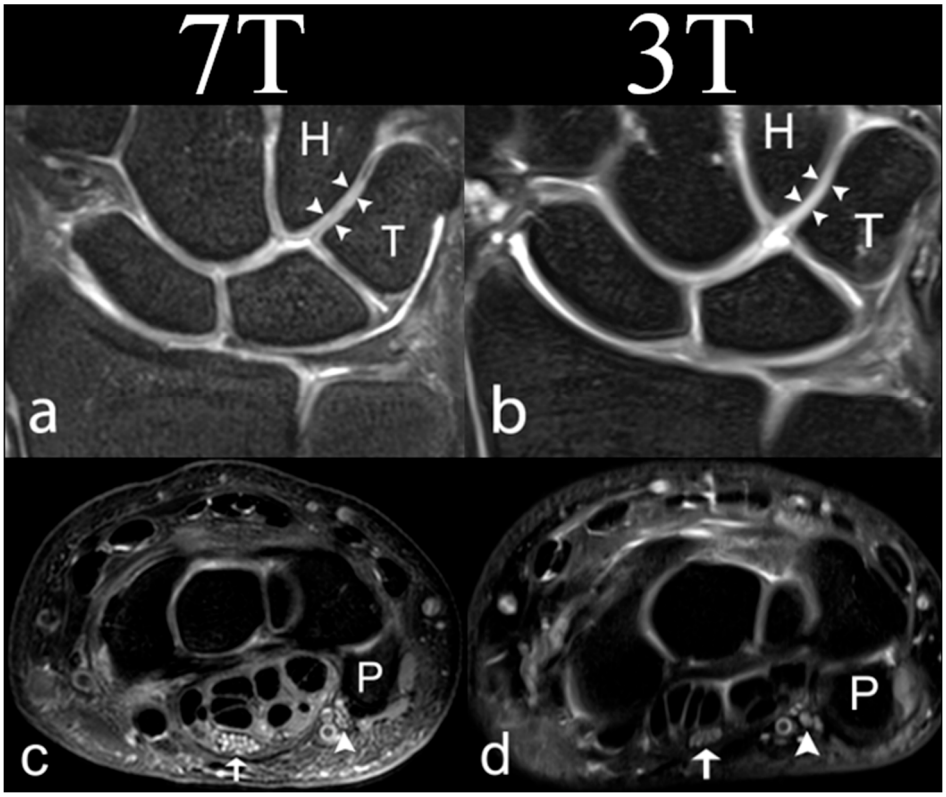

Figure 13. A 39-year-old healthy volunteer. **a** A 7T and (**b**) a 3T coronal 2D PD-weighted section, showing articular cartilage. The arrowheads point to the articular cartilage between the hamate and the triquetrum. **c** A 7T and (**d**) a 3T axial 2D PD-weighted section, showing the median (arrow) and ulnar nerve (arrowhead), at the level of the pisiform bone. *H, hamate; P, pisiform; PD, proton density; T, triquetrum*. Courtesy of European Radiology. 2021, Springer Nature. License CC BY 4.0

This study was the first to compare imaging of the wrist at 7T to 3T using a commercially available wrist coil at 7T. A previous study, using a wrist coil developed for 3T and replicated for use at 7T, did not find a significant difference in visualization of anatomical structures between 7T and 3T[83]. However, only one coronal 2D gradient echo sequence was used for comparison, in contrast with the current study, where five sequences were utilized.

After the publication of this study, a study by Heiss et al. was published comparing image quality of 7T and 3T wrist MRI in 25 participants with chronic wrist pain, with a control group consisting of 25 participants with no wrist pain[126]. They confirmed that image quality was superior at 7T compared to 3T using PD-weighted imaging, when all participants were included in the analysis, but this superiority was not found in the subgroup with chronic wrist pain. Visualization of cartilage was superior at 7T compared to 3T in both groups, but no superiority was found in the depiction of ligaments (the TFCC, the SLL and the LTL).

Paper III

Prior to a scheduled wrist arthroscopy, 7T and 3T MRI was performed in 24 patients with suspected TFCC or SLL injury. Image evaluation was done individually by four musculoskeletal radiologists. The MRI findings were compared with arthroscopy findings. The sensitivity, specificity and accuracy of 7T and 3T MRI were calculated, using wrist arthroscopy as a reference standard. Interobserver and intraobserver agreement were evaluated by intraclass correlation coefficients, where values below 0.50 are interpreted as poor reliability; values between 0.50 and 0.75 as moderate reliability; values between 0.75 and 0.90 as good reliability, and values greater than 0.90 as excellent reliability.

In suspected injury to the TFCC or the SLL, no clear advantage was found using 7T MRI compared to 3T MRI, with wrist arthroscopy as a reference standard (Table 6 and 7). The diagnostic accuracy, at either field strength, was not better than the diagnostic accuracy found in previous studies. Figure 14 shows a TFCC tear, and Figure 15 an SLL tear at both field strengths. At 7T, 82% of TFCC tears and 70% of SLL tears were correctly identified. At 3T, 75% of TFCC tears and 68% of SLL tears were correctly identified.

Table 6. Ranges of the number of tears found on MRI, tears found on arthroscopy, and ranges of true positive, true negative, false positive and false negative found by the four observers for TFCC and SLL tear at 7T and 3T.

Structure	Field Strength	Tear on MRI	Tear on arthroscopy	TP	TN	FP	FN
TFCC	7T	6-15	7	4-7	10-16	2-9	0-2
TFCC	3T	7-12	7	4-6	12-15	3-7	1-3
SLL	7T	6-19	10	5-10	6-15	1-9	0-5
SLL	3T	8-20	10	5-10	6-13	3-10	0-5

FN, false negative; FP, false positive; SLL, scapholunate ligament; T, Tesla; TFCC, triangular fibrocartilage complex; TN, true negative; TP, true positive.

Table 7. Sensitivity, specificity, positive predictive value, negative predictive value, and area under the curve with 95% confidence interval for TFCC and SLL tear at 7T and 3T.

Structure	Field Strength	Sensitivity	Specificity	PPV	NPV	AUC	95% CI for all observers
TFCC	7T	**0.85** (0.67-1.00)	**0.68** (0.53- 0.89)	**0.49** (0.44-0.67)	**0.93** (0.89-1.00)	0.82	0.67-0.94
TFCC	3T	**0.75** (0.57-0.86)	**0.73** (0.63-0.83)	**0.51** (0.46-0.57)	**0.88** (0.83-0.92)	0.77	0.63-0.88
SLL	7T	**0.70** (0.50-1.00)	**0.65** (0.40-0.94)	**0.56** (0.43-0.83)	**0.77** (0.67-1.00)	0.74	0.59-0.89
SLL	3T	**0.69** (0.50-1.00)	**0.55** (0.38-0.81)	**0.48** (0.42-0.63)	**0.74** (0.64-1.00)	0.70	0.52-0.86

AUC, area under the curve; CI, confidence interval; NPV, negative predictive value; PPV, positive predictive value; SLL, scapholunate ligament; T, Tesla; TFCC, triangular fibrocartilage complex.

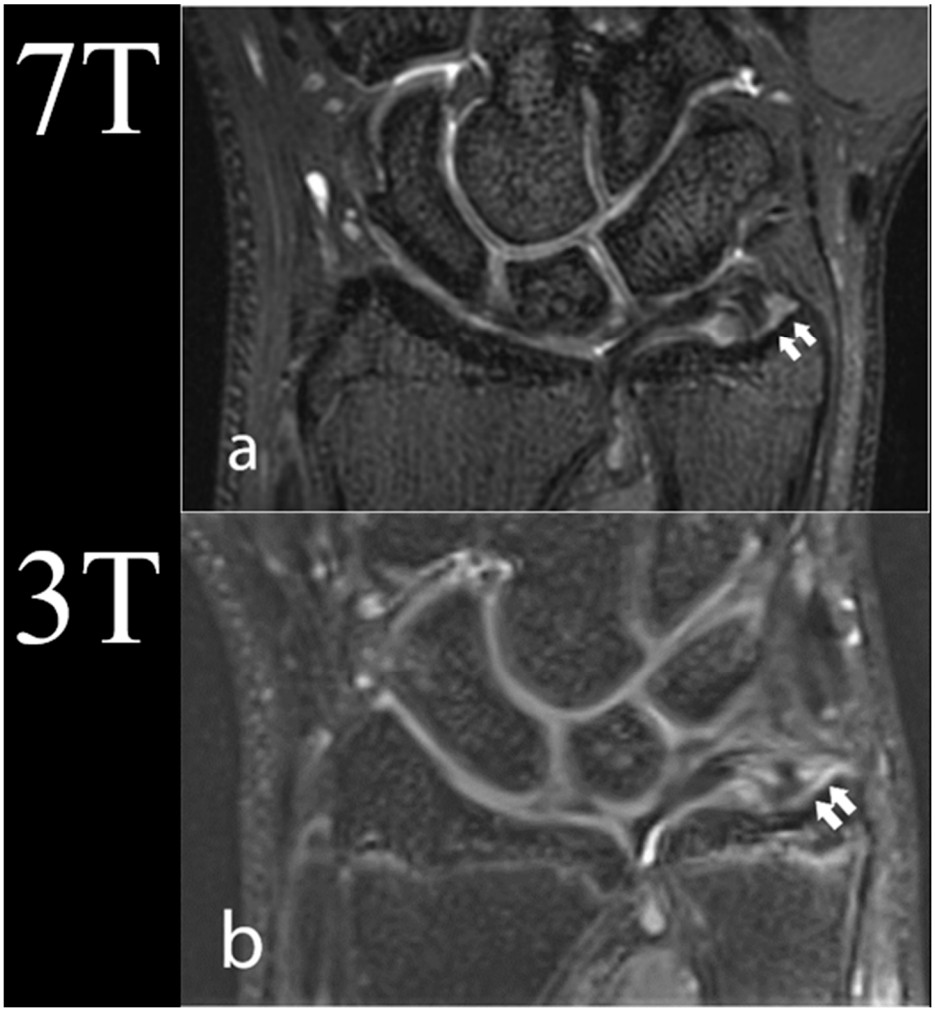

Figure 14. A 19-year-old male with right-sided wrist pain after a sporting accident. MRI showed a clearly delineated TFCC tear at the ulnar styloid (arrows) on coronal reformations at both (**a**) 7T and (**b**) 3T. *T, Tesla; TFCC, triangular fibrocartilage complex.* Courtesy of European Radiology. 2021, Springer Nature. License CC BY 4.0

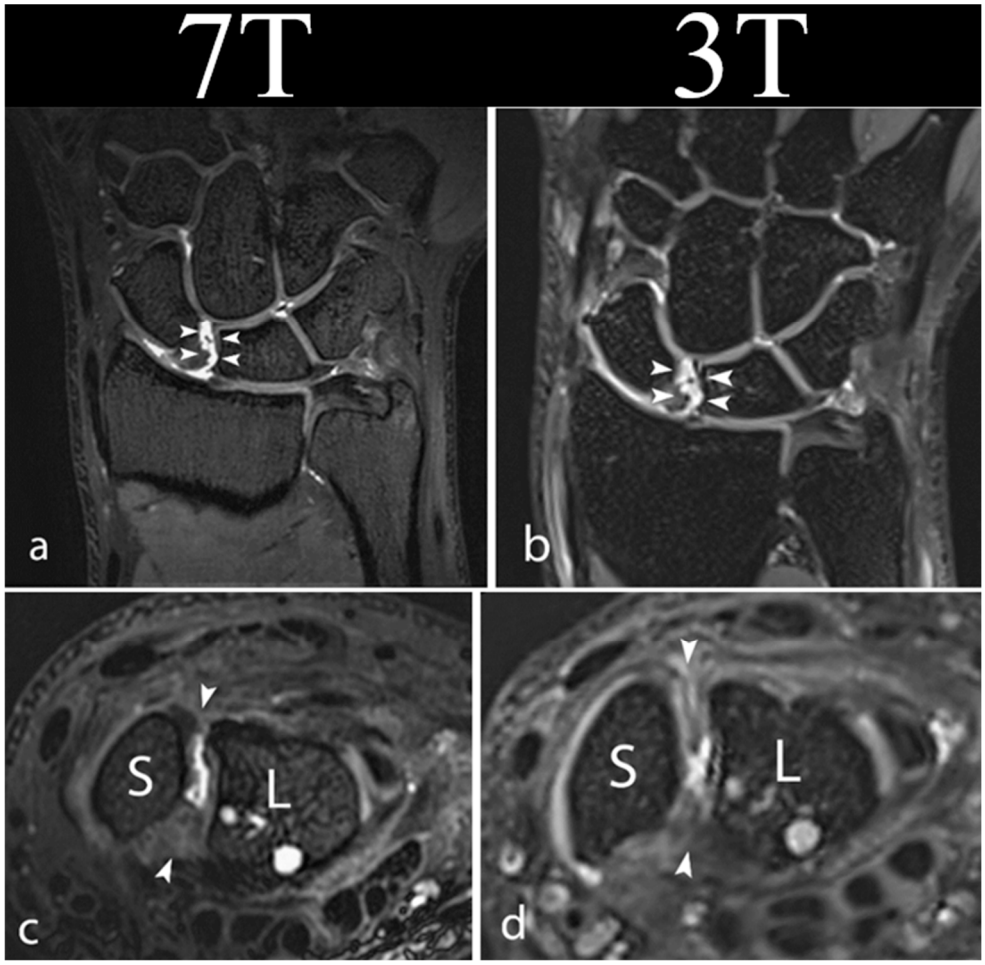

Figure 15. A 24-year-old male with right-sided wrist pain after a work-related injury. MRI showed a clearly delineated SLL tear (arrowheads) on coronal and axial reformations at both (**a, c**) 7T and (**b, d**) 3T. *L, lunate; S, scaphoid; SLL, scapholunate ligament; T, Tesla.* Courtesy of European Radiology. 2021, Springer Nature. License CC BY 4.0

For the TFCC, the interobserver agreement was moderate for both 7T (0.59) and 3T (0.74). Similarly, the interobserver agreement was moderate for both 7T (0.63) and 3T (0.69) with regards to the SLL.

The relatively large variation in the number of found tears between observers, and that only moderate interobserver agreement was achieved for both the TFCC and the SLL at both field strengths, may be caused by differences in experience in musculoskeletal MRI between the observers. It may also be explained by the inherent difficulty in evaluating tears of these small structures with MRI. The findings highlight the importance of using multiple observers in imaging studies.

Apart from ligament tears, other findings of potential clinical importance were made in 14 of the 24 patients. Ganglia were found in 12 patients, subcortical bone cysts in five, old fractures in three, bone marrow oedema in three, tenosynovitis in six, and tendon rupture in two, where one showed a complete rupture of the extensor carpi radialis brevis tendon and one a split rupture of the extensor carpi ulnaris tendon. Regarding some of these findings, particularly ganglia, the MRI report can be of guidance to the arthroscopist. Some of the pathologies are not detectable with arthroscopy, like bone marrow oedema, bone cysts and tendon ruptures. Other examples of lesions not detectable using arthroscopy are degenerative conditions, tumours, and ligament tears in compartments not accessed during arthroscopy[133].

In summary, a majority of TFCC and SLL tears can be found using MRI at 7T and 3T, but MRI cannot replace wrist arthroscopy as the reference standard. Utilizing a higher field strength (i.e. 7T) does not in itself improve diagnostic accuracy. Heiss et al. likewise found no superiority of 7T compared to 3T MRI in wrist ligament imaging in healthy participants or participants with chronic wrist pain[126]. However, their study did not include a comparison with wrist arthroscopy findings. Despite not reaching the diagnostic accuracy of wrist arthroscopy in the evaluation of wrist ligaments, MRI plays an important complimentary role in the evaluation of patients with wrist pain.

Paper IV

A clinical wrist examination and an MRI were performed on 13 patients who had been treated with SLL reconstruction 4-13 years priorly to restore scapholunate alignment, improve function and lessen pain. Briefly, the reconstructions used in this study consisted of an autograft (the flexor carpi radialis tendon) pulled through bone tunnels in the scaphoid and the lunate and fixated with interference screws made of biocomposite material. The MRI protocol included a new 3D sequence, optimized for wrist ligament visualization, in addition to clinical routine wrist MRI sequences. The clinical examination was performed by a senior hand surgeon and the image evaluation was carried out in consensus by two senior radiologists.

Only one of the 13 evaluated grafts was found intact on MRI. In all other patients, the reconstruction grafts were absent, and bone marrow had replaced the graft in at least one of the tunnels through the scaphoid or the lunate. Other notable MRI findings were scapholunate dissociation in 10 (77%) and an increased scapholunate angle in 11 (85%) of the patients, indirectly indicating loss of graft integrity. Extensive osteoarthritis was found in two (15%) of the patients, who also presented with subluxation of the lunate bone. There were no signs of osteolysis around the bore canals in any of the patients. Results from the MR examinations for all patients is detailed in Table 8.

Table 8. MRI results in 13 patients with scapholunate ligament reconstruction. SL dissociation is defined when the distance is >2,5 mm. An increased SL angle is >62,5°.

Years since surgery	Intact graft	SL distance (mm)	SL-angle (°)	Bone marrow filling in bore canal	Thinning of articulate cartilage	Bone marrow oedema	Extensive osteo-arthritis
12	No	5,95	78,6	L	S,L,R	-	No
10	No	6,20	65,4	S,L	S,L,R	S,L,R,C	Yes
13	No	1,85	48,5	L	-	-	No
4	No	4,15	76,4	L	-	-	No
8	No	4,78	87,2	S	S,L	S,L,R,H	Yes
6	Yes	3,00	63,4	-	-	S,R	No
8	No	1,25	73,4	S	S,L	S,L	No
5	No	5,20	50,7	S,L	S	-	No
5	No	5,03	72,7	S	S	S,R	No
4	No	4,35	87,3	L	-	-	No
4	No	2,89	81,3	L	-	-	No
5	No	0,93	67,5	S,L	-	-	No
9	No	3,32	62,7	L	S	-	No

C, capitatum; H, hamatum; L, lunate; MRI, magnetic resonance imaging; N/A, not applicable; R, radius; S, scaphoid; SL, scapholunate.

Selected results from the clinical examinations are detailed in Table 9. Self-reported functional assessment showed improvement in DASH and PRWE scores in all but one of the patients compared to preoperative values (although data was missing for DASH in one patient, for PRWE in two patients). The findings were statistically significant. Only a minority reported pain intensity above the “mild” range during activity using the visual analogue scale (VAS), where ratings of 0-4 mm were considered as representing no pain, 5-44 mm mild pain, 45-74 mm moderate pain and 75-100 mm severe pain. There was a statistically significant reduction of mobility in flexion, extension and radial deviation on the operated side compared to the healthy side. No apparent association between the imaging- and clinical findings was found.

Table 9. Some of the results from the clinical follow up examination after surgery, prior to MRI in 13 patients with scapholunate ligament reconstruction. A positive DASH score and a positive PRWE score indicate an improved disability score of the affected extremity and an improved disability score of the affected wrist, respectively, compared to the scores registered prior to surgery. VAS ratings of 0-4 mm were considered as representing no pain, 5-44 mm mild pain, 45-74 mm moderate pain and 75-100 mm severe pain. A (-) indicates that data is missing.

Years since surgery	DASH difference (points)	PRWE difference (points)	VAS (rest)	(VAS active)
12	58	-	0	0
10	25	36	3	15
13	2	33	0	10
4	50	64,5	4	8
8	-29	-13,5	32	72
6	27	11	30	78
8	7	29	0	30
5	42	40	2	30
5	20	32	12	60
4	6	30	35	35
4	-	-	18	77
5	8	14	20	20
9	17	15	0	2

DASH, Disabilities of arm, shoulder and hand questionnaire; kg, kilograms; MRI, magnetic resonance imaging; PRWE, patient-rated wrist evaluation; VAS, visual analogue scale.

Figure 16 shows the only intact scapholunate ligament reconstruction graft found on MRI, visualized on the dorsal side and in the bore canal through the lunate. Figure 17 shows bone marrow replacement of the bore canal in the scaphoid, subluxation of the lunate and SL-dissociation.

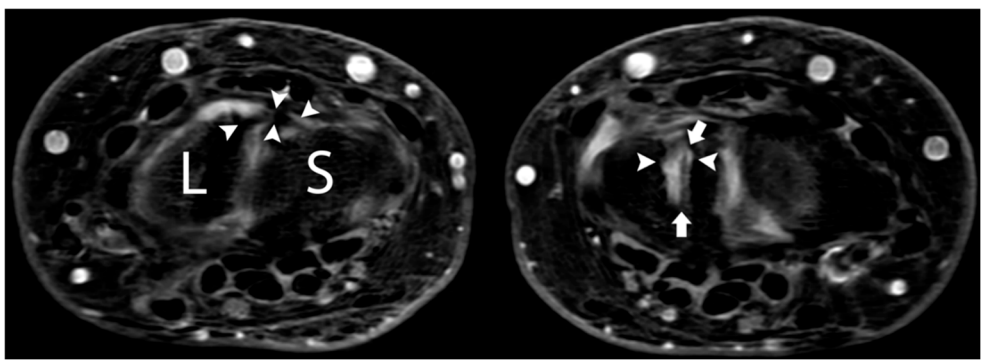

Figure 16. A 50-year-old female with 3T MRI performed six years after SLL reconstruction. The image on the left shows an axial, PD-weighted Dixon TSE sequence with an intact reconstruction graft dorsally (arrowheads). The image on the right, using the same MR sequence, shows a slight widening of the bore canal in the lunate where the bioabsorbable screw was before resorption (arrowheads). The intact reconstruction graft passes through the canal (arrows). *L, lunate; MRI, magnetic resonance imaging; PD, proton density; S, scaphoid; SLL, scapholunate ligament; T, Tesla; TSE, turbo spin echo.*

Figure 17. A 65-year-old male with 3T MRI performed 10 years after SLL reconstruction. A coronal T1-weighted sequence shows almost complete bone marrow replacement of the bore canal in the scaphoid (arrowheads). There was also partial replacement of the bore canal with bone marrow in the lunate but not present in this image slice (arrow). Notice the SL-dissociation and the ulnar subluxation of the lunate. *MRI, magnetic resonance imaging; SL, scapho-lunate; SLL, scapholunate ligament; T, Tesla*

In this study, the only intact graft was clearly visualized at 3T MRI. The absence of a visible graft in the other patients was interpreted as true graft loss rather than poor visualization. The utilized graft has a larger diameter than the native SLL, and it should be clearly delineated using a 3D sequence. Also, no fibrous tissue was seen at its expected location. The replacement with bone marrow in at least one of the bore tunnels in all patients without an intact graft also shows that the graft was not present in these tunnels. Despite scapholunate dissociation, an increased scapholunate angle, absence of an intact graft and various degrees of degenerative changes, most patients showed a good functional outcome after surgery, indicated

by an improvement of DASH and PRWE scores. The limited number of patients make caution necessary in generalizing these results. However, the findings corroborate previous findings, where radiographs showed scapholunate dissociation, increased scapholunate angle and signs of degradation in patients with good functional outcome several years after reconstruction of the SLL[18].

Thus, using MRI in the follow-up after reconstruction of the SLL provides information regarding graft integrity that cannot be achieved with clinical examination and radiographs. MRI findings could inform hand surgeons about differences in graft integrity after various reconstructive techniques. This could affect preference between different reconstructive techniques. Improvement in functionality is, of course, an important follow-up parameter, but it is not known whether functionality would deteriorate after a longer follow-up period in patients where the SLL reconstruction is not intact.

Conclusions

Magnetic resonance imaging is a valuable diagnostic tool in patients with suspected wrist ligament injury, and it contributes with information not available by wrist arthroscopy. However, in suspected wrist ligament injury, it still does not reach the same diagnostic accuracy as wrist arthroscopy even when a 3D sequence is added to the MRI protocol, or when the field strength is increased to 7T. In the follow-up after SLL reconstruction, MRI contributes with valuable information regarding graft integrity.

Paper I

A 3D sequence can replace 2D sequences in the assessment of wrist ligaments at 3T MRI.

Paper II

In the absence of pathology, anatomical structures of the wrist are better visualized at 7T than at 3T MRI.

Paper III

When wrist ligament injury is suspected, MRI at 7T was not superior to MRI at 3T. MRI is a valuable complementary tool to wrist arthroscopy.

Paper IV

Using MRI in the follow-up after SLL reconstruction contributes valuable information regarding graft integrity.

Future aspects

In musculoskeletal MRI, 3D imaging is underutilized. The thinner slices and possibility for MPR to improve the visualization of intricate structures can result in a more confident assessment by the radiologist. The 3D sequence developed for 3T as a part of this thesis is currently being clinically tested and implemented at our facility for indications other than just wrist ligament injury. The 3D sequence can potentially replace the three 2D PD-weighted sequences in our clinical protocol, thus shortening the total acquisition time. The fourth study of this thesis was conducted at the Sahlgrenska University Hospital in Gothenburg, where a 3D sequence was built using the sequence developed in Lund as a template and an inspiration. Use of this sequence in clinical protocols is currently being implemented.

As the diagnostic accuracy of MRI at 7T in suspected wrist ligament injury never had been investigated prior to this thesis, we choose to use a completely non-invasive approach. As previously mentioned, wrist MRA has previously been found superior to MRI in detecting wrist ligament injuries at lower field strengths, and it would be of great interest to investigate both indirect and direct wrist MRA at 7T.

Ultrasound is a low cost, non-invasive, dynamic modality with great availability. However, it is operator dependent, and it cannot depict structures obscured by bones. Using a high frequency, linear transducer, the TFCC, the SLL and the LTL can be visualized using ultrasound[134], and injury should be suspected if ligament fibres are discontinuous, or if a ligament is not seen in its expected anatomical location[135]. Ultrasound examination of the wrist can be performed during clinical examination by a trained hand surgeon, alternatively by a musculoskeletal radiologist. The sensitivity, specificity and accuracy of wrist ultrasound can thus easily be investigated, using wrist arthroscopy as a reference standard.

In recent years, research on dynamic MRI of the wrist has been conducted, as it may have the potential of assessing altered wrist kinematics in patients with wrist ligament injury[136–138]. If this will lead to clinically practical implications remains to be seen.

In follow-up studies after reconstructive surgery of the SLL, X-ray imaging is usually the only imaging modality utilized[51,139]. With its ability to depict soft tissues in detail, MRI could be a valuable tool in future follow-up studies after wrist ligament reconstructive surgery, to better assess graft integrity and potential complications. This would facilitate comparison between different surgical techniques based on differences in long-term graft integrity as seen on MRI.

Acknowledgements

Ett stort tack till alla er som har hjälpt mig under min doktorandresa!

Min ursprungliga huvudhandledare Mats Geijer, som föreslog att jag skulle ta mig an detta projekt, och som har varit ett enormt stöd för mig under hela vägen. Du har fått stå ut med många telefonsamtal även sena kvällar och helger, och alltid gett mig snabb och värdefull feedback. Du har varit min klippa.

Min nuvarande huvudhandledare Erik Hedström, som antog uppgiften med bravur efter att Mats blivit professor vid Göteborgs Universitet. Stort tack för att du hjälpte mig i mål! Du har alltid varit en god vän och ett stort stöd.

Min bihandledare Anders Björkman, som möjliggjorde projektet med forskningsmedel till handledsspolen till 7T och som har varit med och format projektet sedan start. Du har kontinuerligt bistått med en handkirurgs perspektiv, och tålmodigt förklarat för mig. Du har givit min forskning en bredd och mångsidighet. Även ett stort tack för att jag fick vara med vid en artroskopi!

Min bihandledare Magnus Flondell, som möjliggjorde att projektet kunde fortsätta när Anders blev professor i Göteborg. Du blev min fasta kontakt på handkirurgen, och utan dig hade vi aldrig kunnat fullfölja det essentiella tredje delarbetet.

Mina kära medförfattare, som utöver handledare och bihandledare var Isabella Björkman-Burtscher, Rana Ab-Fawaz, Ingvar Kristiansson, Björn Lundin, Elenya Aksyuk, Pawel Szaro, Karin Markenroth Bloch, Rami Abu Shalhoub och Maria Zander. Jag är mycket tacksam för ert arbete, ert engagemang och er input.

MR-fysiker Jimmy Lätt och Peter Mannfolk. Ni har utgjort oumbärlig expertis i sekvensutveckling och sekvensoptimering vid 3T. Ni har även tålmodigt besvarat mina frågor så att jag uppnått en bättre förståelse för sekvenserna.

MR-fysiker Karin Markenroth. Vi arbetade många timmar tillsammans med sekvensutvecklingen vid 7T. Ärligt talat var det du som gjorde jobbet, jag tyckte mest till om bilderna. Jag imponeras fortsatt över dina kunskaper och ditt tålamod, och tycker dessutom att det var ett väldigt roligt och givande att arbeta med dig. Även ett stort tack för ditt stöd när jag presenterade vid ISMRMs konferens i Dubrovnik, och att du fortsatt hjälper mig när jag inte helt förstår MR-fysiken.

MR-fysiker Fredy Visser vid Utrecht Universitet. Tack för att du hjälpte oss i mål med sekvensutvecklingen vid 7T.

Maria Zander, handkirurg och doktorand vid Göteborg Universitet. Tack för ett fint samarbete med det fjärde delarbetet. Det var ett sant nöje att skriva tillsammans med dig. Jag uppskattar att du var med under en stor del av bildgranskningen i projektet.

Mina kära kollegor på barnröntgen Kristina Vult von Steyern, Fredrik Stålhammar, Pär Wingren, Marie Wiklund, Nicole McMichael, Sofie Meyer, Gylfi Asbjörnsson, Fabian van de Bunt och Erik Hedström. Ni har uppvisat enorm förståelse och givit mig ert stöd som har möjliggjort min forskning. Jag älskar att arbeta tillsammans med er; ni är min familj på jobbet. Ett särskilt tack till Kristina, som har varit min mentor.

Magnus Båth, professor och sjukhusfysiker i Göteborg. Utöver att ha skapat VGC Analyzer, som utgjorde den ”statistiska kärnan” i två av avhandlingens delarbeten, har du även personligen besvarat mina frågor om metoden och applikationen av densamma i mina delarbeten. Jag är mycket tacksam.

Peter Hochbergs, min chef. Du har alltid prioriterat forskning och vidareutbildning högt. Att veta att du alltid är öppen och stödjande för sådant som leder till utveckling är något jag verkligen uppskattar. Utan dig hade forskning vid Bild- och Funktionsavdelningen varit mycket svårare att genomföra.

Professor Pia Maly Sundgren. Din auktoritet och styrka placerar oss på kartan inom forskningsvärlden, och du har hjälpt mig när jag stötte på svårigheter längs vägen. Tack på förhand för att du är ordförande vid min disputation!

Ett stort tack till alla MR-sköterskor som har ställt upp med att utföra MR-undersökningarna. Er skicklighet och ert vänliga stöd har varit oumbärligt. Ett särskilt tack till Edward Boncina, Linda Wennberg, Boel Hansson, Matilda Bergsten, Susanne Nilsson, Ylva Brogren, Adela Hodzik och Noinar Phoemsawang.

Titti Owman. Din positiva energi och ditt uppriktiga stöd till min forskning har varit en inspirationskälla.

Operationskoordinatorerna Christina Svensson och Angelika Frome Walker vid handkirurgen på SUS. När inklusionen av patienter vid det tredje arbetet försvårandes, av många anledningar, fick vi etablerat ett personligt och fint samarbete, där ni med er kompetens och ert engagemang bistod mig på ett fantastiskt sätt. Jag är mycket tacksam!

Vigith, min hustru. Det var du som övertalade mig att acceptera detta projekt. Utan dig hade denna avhandling inte skrivits, och jag hade nog aldrig disputerat. Tack för att du har möjliggjort denna resa och stått vid min sida!

Mina barn Julian, Anna och Evelina. Ni har distraherat mig från min forskning, vilket har gett mig behövliga pauser. Ni påminner mig om att arbete och forskning inte är det enda som är viktigt.

Mina föräldrar Ingemar and Elisabeth. Ni har alltid trott på mig, och gett mig självförtroendet att ta mig an svåra uppgifter. Tack för er obetingade kärlek.

Min bror David. När jag efter AT inte hade en aning om vad jag skulle använda min läkarutbildning till föreslog du att jag skulle överväga radiologi. Jag hade inte alls tänkt på det som en möjlighet, och är tacksam för att du ledde in mig på spåret till min drömspecialitet, som jag hädanefter såg som det självklara valet för mig. Utan ditt inflytande hade jag knappt vetat vad MR var.

Min syster Maria. Tack för din kärlek.

Min kusin och nära vän Johan. Du påbörjade din doktorandresa några år innan mig, och har varit ett stöd och en klok rådgivare längs vägen. Tack!

Mine studiekamrater fra lægestudiet Adam, Anne, Hans Henrik och Simon. Vores venskab og vores samarbejde under lægestudiet i København, og KBU i Aalborg (Simon), har været med til at forme mig faglig og personlig. Jag sætter stor pris på vores venskab, og holder minderne vi skabt sammen varmt om hjertet. Takket være jer bliver jeg ved med at lave sprogelige fejl når jeg skriver på svensk, hvilket jeg selv synes giver mine tekster et personlig præg, og har bragt min vejleder Mats (som også, til dels, er danskere) meget underholdning. Jeg lover dog at jeg sgu er stoppet med att tilbyde folk en skid i kaffen.

Jag vill även tacka övriga vänner, familjemedlemmar och kollegor som har intresserat sig för min forskning, och (åtminstone artigt låtsats) lägga örat till när jag haft långa utläggningar om vad jag sysslar med – särskilt tack till Anders Holm, David Nummi, Daniel och Dibisa Singam Wendel och min kära mormor Karin Linderoth.

Under skrivandet av såväl kappa som manuskript har musik utgjort en viktig källa för inspiration och stämningsskapande fokus för mig. Jag vill särskilt nämna soundtracket som skapats av Keiichi Okabe, till spelet NieR Automata, som varit en trogen följeslagare sedan det släpptes 2017. Annan musik som inspirerat mig under skrivandet har varit Deftones, the Cure, Keygen Church, Paysage D´Hiver och stämningsmusik från spelserierna Castlevania, Final Fantasy, Silent Hill och Ōkami.

References

1. Kijima Y, Viegas SF (2009) Wrist anatomy and biomechanics. *J Hand Surg Am*. 34:1555-1563
2. Davis KW, Blankenbaker DG (2009) Imaging the ligaments and tendons of the wrist. *Semin Roentgenol*. 45:194-217
3. Chan JJ, Teunis T, Ring D (2014) Prevalence of triangular fibrocartilage complex abnormalities regardless of symptoms rise with age: systematic review and pooled analysis. *Clin Orthop Relat Res*. 472:3987-3994
4. Sanderson M, Mohr B, Abraham MK (2020) The emergent evaluation and treatment of hand and wrist injuries: an update. *Emerg Med Clin North Am*. 38:61-79
5. Lehman JD, Krishnan KR, Stepan JG, Nwachukwu BU (2020) Prevalence and treatment outcomes of hand and wrist injuries in professional athletes: a systematic review. *HSS J*. 16:280-287
6. Mespreuve M, Vanhoenacker F, Verstraete K (2015) Imaging findings of the distal radio-ulnar joint in trauma. *J Belgian Soc Radiol*. 99:1-20
7. Palmer AK, Werner FW (1981) The triangular fibrocartilage complex of the wrist - anatomy and function. *J Hand Surg Am*. 6:153-162
8. Watson HK, Black DM (1987) Instabilities of the wrist. *Hand Clin*. 3:103-111
9. Hermann BF (2006) Ligament injuries of the hand and wrist. *Clin Occup Environ Med*. 5:323-331
10. Connell D, Page P, Wright W, Hoy G (2001) Magnetic resonance imaging of the wrist ligaments. *Australas Radiol*. 45:411-422
11. Schmauss D, Pöhlmann S, Lohmeyer JA, Germann G, Bickert B, Megerle K (2016) Clinical tests and magnetic resonance imaging have limited diagnostic value for triangular fibrocartilaginous complex lesions. *Arch Orthop Trauma Surg*. 136:873-880
12. Hafezi-Nejad N, Carrino JA, Eng J, et al. (2016) Scapholunate interosseous ligament tears: diagnostic performance of 1.5 T, 3 T MRI, and MR arthrography - a systematic review and meta-analysis. *Acad Radiol*. 23:1091-1103
13. Ahsan ZS, Yao J (2012) Complications of wrist arthroscopy. *Arthrosc - J Arthrosc Relat Surg*. 28:855-859
14. De Smet L (2002) Pitfalls in wrist arthroscopy. *Acta Orthop Belg*. 68:325-329
15. Reiser D, Hedspång M, Sagerfors M (2024) NanoScope wrist arthroscopy under wide-awake local anesthesia with no tourniquet: a prospective series of 30 consecutive patients. *J Hand Microsurg*. 16:100067

16. Mohamadi A, Claessen FMAP, Ozkan S, Kolovich GP, Ring D, Chen NC (2017) Diagnostic wrist arthroscopy for nonspecific wrist pain. *Hand*. 12:193-196
17. Andersson JK, Andernord D, Karlsson J, Fridén J (2015) Efficacy of magnetic resonance imaging and clinical tests in diagnostics of wrist ligament injuries: a systematic review. *Arthrosc - J Arthrosc Relat Surg*. 31:2014-2020
18. Goeminne S, Borgers A, van Beek N, De Smet L, Degreef I (2021) Long-term follow-up of the three-ligament tenodesis for scapholunate ligament lesions: 9-year results. *Hand Surg Rehabil*. 40:448-452
19. Friedrich KM, Komorowski A, Trattnig S (2012) 7T imaging of the wrist. *Semin Musculoskelet Radiol*. 16:88-92
20. Sasao S, Beppu M, Kihara H, Hirata K, Takagi M (2003) An anatomical study of the ligaments of the ulnar compartment of the wrist. *Hand Surg*. 8:219-226
21. Flores D V., Umpire DF, Rakhra KS, Jibri Z, Belmar GAS (2023) Distal radioulnar joint: normal anatomy, imaging of common disorders, and injury classification. *Radiographics*. 43
22. Kirchberger MC, Unglaub F, Mühldorfer-Fodor M, et al. (2015) Update TFCC: histology and pathology, classification, examination and diagnostics. *Arch Orthop Trauma Surg*. 135:427-437
23. Berger RA (1996) The gross and histologic anatomy of the scapholunate interosseous ligament. *J Hand Surg Am*. 21:170-178
24. Ritt MJ, Bishop a T, Berger R a, Linscheid RL, Berglund LJ, An KN (1998) Lunotriquetral ligament properties: a comparison of three anatomic subregions. *J Hand Surg Am*.23:425-431
25. Berger RA, Imeada T, Berglund L, An KN (1999) Constraint and material properties of the subregions of the scapholunate interosseous ligament. *J Hand Surg Am*. 24:953-962
26. Watanabe A, Souza F, Vezeridis PS, Blazar P, Yoshioka H (2010) Ulnar-sided wrist pain. II. Clinical imaging and treatment. *Skeletal Radiol*. 39:837-857
27. Shahabpour M, Abid W, van Overstraeten L, van Royen K, de Maeseneer M (2021) Extrinsic and intrinsic ligaments of the wrist. *Semin Musculoskelet Radiol*. 25:311-328
28. Shahabpour M, Staelens B, Van Overstraeten L, et al. (2015) Advanced imaging of the scapholunate ligamentous complex. *Skeletal Radiol*. 44:1709-1725
29. Palmer AK (1989) Triangular fibrocartilage complex lesions: a classification. *J Hand Surg Am*. 14:594-606
30. Abe Y, Tominaga Y, Yoshida K (2012) Various patterns of traumatic triangular fibrocartilage complex tear. *Hand Surg*. 17:191-198
31. Ng AWH, Griffith JF, Fung CSY, et al. (2017) MR imaging of the traumatic triangular fibrocartilaginous complex tear. *Quant Imaging Med Surg*. 7:443-460
33. Geissler WB, Freeland AE, Savoie FH, McIntyre LW, Whipple TL (1996) Intracarpal soft-tissue lesions associated with an intra-articular fracture of the distal end of the radius. *J Bone Joint Surg Am*. 78:357-365

34. Andersson JK, Garcia-Elias M (2013) Dorsal scapholunate ligament injury: a classification of clinical forms. *J Hand Surg Eur Vol*. 38:165-169
35. Baker A, Whipple TL, Poehling GG, Bain GI (2021) History of Wrist Arthroscopy. *Arthrosc Endosc Elbow, Wrist Hand Surg Anat Tech*. 15-43
34. Unger T, Anand P (2023) Wrist Arthroscopy. StatPearls Publishing
35. Atzei A, Luchetti R, Carletti D, Marcovici LL, Cazzoletti L, Barbon S (2021) The hook test is more accurate than the trampoline test to detect foveal tears of the triangular fibrocartilage complex of the wrist. *Arthrosc - J Arthrosc Relat Surg*. 37:1800-1807
36. Greene R, Kakar S (2017) The suction test: a novel technique to identify and verify successful repair of peripheral triangular fibrocartilage complex tears. *J Wrist Surg*. 6:334-335
37. Atzei A, Luchetti R (2011) Foveal TFCC tear classification and treatment. *Hand Clin*. 27:263-272
38. Messina NA, Dowley KS, Raducha JE, Gil JA (2023) Radial sided triangular fibrocartilage complex tears: a comprehensive review. *Hand*. 18:1245-1252
39. Mathoulin C (2016) Treatment of dynamic scapholunate instability dissociation: contribution of arthroscopy. *Hand Surg Rehabil*. 35:377-392
40. Krastman P, Mathijssen NMC, Bierma-Zeinstra SMA, Kraan GA, Runhaar J (2020) Diagnostic accuracy of history taking, physical examination and imaging for non-chronic finger, hand and wrist ligament and tendon injuries: a systematic review update. *BMJ Open*. 10:1-12
41. Athlani L, Cholley-Roulleau M, Blum A, Teixeira PAG, Dap F (2023) Intercarpal arthrodesis: a systematic review. *Hand Surg Rehabil*. 42:93-102
42. van Kampen RJ, Henk Coert J, Moran SL (2024) Mid-term outcomes of three commonly used surgical reconstructions for scapholunate instability. *J Hand Surg Eur Vol*. 49:852-858
43. Haerle M, Schmelzer-Schmied N, Lampert FM (2023) Arthroscopic Capsulodesis for the Treatment of Dynamic Scapholunate Dissociations. *Tech Hand Up Extrem Surg*. 27:95-99
44. Cuénod P, Charrière E, Papaloïzos MY (2002) A mechanical comparison of bone-ligament-bone autografts from the wrist for replacement of the scapholunate ligament. *J Hand Surg Am*. 27:985-990
45. Athlani L, Pauchard N, Detammaecker R, et al. (2018) Treatment of chronic scapholunate dissociation with tenodesis: a systematic review. *Hand Surg Rehabil*. 37:65-76
46. Rosenwasser MP, Miyasajsa KC, Strauch RJ (1997) The RASL Procedure. *Tech Hand Up Extrem Surg*. 1:263-272
47. Solgård L, Gvozdenovic R (2024) Single- and bicolumn limited intercarpal fusion: a solution for the SLAC or SNAC wrist. *J Wrist Surg*. 13:16-23
48. Kakar S, Greene RM, Denbeigh J, Van Wijnen A (2019) Scapholunate ligament internal brace 360 tenodesis (SLITT) procedure: a biomechanical study. *J Wrist Surg*. 8:250-254

49. Brunelli GA, Brunelli GR (1995) A new technique to correct carpal instability with scaphoid rotary subluxation: a preliminary report. *J Hand Surg Am*. 20:82-85
50. Garcia-Elias M, Lluch AL, Stanley JK (2006) Three-ligament tenodesis for the treatment of scapholunate dissociation: indications and surgical technique. *J Hand Surg Am.* 31:125-134
51. Daly LT, Daly MC, Mohamadi A, Chen N (2020) Chronic scapholunate interosseous ligament disruption: a systematic review and meta-analysis of surgical treatments. *Hand*. 15:27-34
52. Corella F, Del Cerro M, Ocampos M, Simon de Blas C, Larrainzar-Garijo R (2017) Arthroscopic scapholunate ligament reconstruction, volar and dorsal reconstruction. *Hand Clin*. 33:687-707
53. Talwalkar SC, Edwards ATJ, Hayton MJ, Stilwell JH, Trail IA, Stanley JK (2006) Results of tri-ligament tenodesis: a modified brunelli procedure in the management of scapholunate instability. *J Hand Surg Am*. 31:110-117
54. Rehnitz C, Klaan B, von Stillfried F, et al. (2016) Comparison of modern 3D and 2D MR imaging sequences of the wrist at 3 Tesla. *RöFo - Fortschritte auf dem Gebiet der Röntgenstrahlen und der Bildgeb Verfahren*. 188:753-762
55. Reavey PL, Hammert WC (2021) Examination of the Wrist. *Plast Reconstr Surg*. 147:284e-294e
56. Hindman BW, Kulik WJ, Lee G, Avolio RE (1989) Occult fractures of the carpals and metacarpals: demonstration by CT. *Am J Roentgenol*. 153:529-532
57. Pérez-Úbeda MJ, Urbina-Balanz A, Rizo B, Collado-Gosálvez A, Gimeno MD, Marco-Martinez F (2022) Association between hounsfield units in preoperative wrist computed tomography scans and outcomes after wrist fracture surgery. *Indian J Orthop*. 56:2141-2152
58. Tiegs-Heiden CA, Howe BM (2020) Imaging of the hand and wrist. *Clin Sports Med*. 39:223-245
59. Sabbagh MD, Morsy M, Moran SL (2019) Diagnosis and management of acute scaphoid fractures. *Hand Clin*. 35:259-269
60. Nüsslin F. Wilhelm (2020) Conrad Röntgen: the scientist and his discovery. *Phys Medica*. 79:65-68
61. Stevenson M, Levis JT (2019) Image diagnosis: scapholunate dissociation. *Perm J*. 23:4-5
62. Fotiadou A, Patel A, Morgan T, Karantanas AH (2011) Wrist injuries in young adults: the diagnostic impact of CT and MRI. *Eur J Radiol*. 77:235-239
63. Kessler I, Silberman Z (1961) An experimental study of the radiocarpal joint by arthrography. *Surg Gynecol Obstet*. 112:33-40
64. Linkous MD, Gilula LA (1998) Wrist arthrography today. *Radiol Clin North Am*. 36:651-672
65. Bhattacharyya K (2016) Godfrey Newbold Hounsfield (1919-2004): the man who revolutionized neuroimaging. *Ann Indian Acad Neurol*. 19:448-450
66. Malshikare VA, Jerome JTJ (2023) Computed tomographic arthrography (arthroscanner) of the wrist joint: why, how, and when. *Indian J Orthop*. 57:930-937

67. Koskinen SK, Haapamäki VV, Salo J, et al. (2013) CT arthrography of the wrist using a novel, mobile, dedicated extremity cone-beam CT (CBCT). *Skeletal Radiol*. 42:649-657
68. Bille B, Harley B, Cohen H (2007) A comparison of CT arthrography of the wrist to findings during wrist arthroscopy. *J Hand Surg Am*. 32:834-841
69. Smith HJ (2021) The history of magnetic resonance imaging and its reflections in Acta Radiologica. *Acta radiol*. 62:1481-1498
70. Xia Y, Stilbs P (2016) The first study of cartilage by magnetic resonance: a historical account. *Cartilage*. 7:293-297
71. Moser E, Stadlbauer A, Windischberger C, Quick HH, Ladd ME (2009) Magnetic resonance imaging methodology. *Eur J Nucl Med Mol Imaging*. 36:30-41
72. Sadleir R, Minhas AS (2022) Electrical properties of tissues - quantitative magnetic resonance mapping. *Adv Exp Med Biol.* 1380:1-206
73. Van De Moortele PF, Akgun C, Adriany G, et al. (2005) B1 destructive interferences and spatial phase patterns at 7 T with a head transceiver array coil. *Magn Reson Med*. 54:1503-1518
74. Hidalgo-Tobon SS (2010) Theory of gradient coil design methods for magnetic resonance imaging. *Concepts Magn Reson Part A Bridg Educ Res*. 36:223-242
75. Gruber B, Froeling M, Leiner T, Klomp DWJ (2018) RF coils: a practical guide for nonphysicists. *J Magn Reson Imaging*. 48:590-604
76. Hansen MS, Kellman P (2015) Image reconstruction: an overview for clinicians. *J Magn Reson Imaging*. 41:573-585
77. Kwok WE (2022) Basic Principles of and Practical Guide to Clinical MRI Radiofrequency Coils. *Radiographics*. 42:898-918
78. Friedrich KM, Chang G, Vieira RLR, et al. (2009) In vivo 7.0-tesla magnetic resonance imaging of the wrist and hand: technical aspects and applications. *Semin Musculoskelet Radiol*. 13:74-84
79. Radue EW, Weigel M, Wiest R, Urbach H (2016) Introduction to magnetic resonance imaging for neurologists. *Contin Lifelong Learn Neurol*. 22:1379-1398
80. Bangerter NK, Taylor MD, Tarbox GJ, Palmer AJ, Park DJ (2016) Quantitative techniques for musculoskeletal MRI at 7 Tesla. *Quant Imaging Med Surg*. 6:715-730
81. Juras V, Mlynarik V, Szomolanyi P, Valkovič L, Trattnig S (2019) Magnetic resonance imaging of the musculoskeletal system at 7T: morphological imaging and beyond. *Top Magn Reson Imaging*. 28:125-135
82. Metzger GJ, Snyder C, Akgun C, Vaughan T, Ugurbil K, Van De Moortele PF (2008) Local B1+ shimming for prostate imaging with transceiver arrays at 7T based on subject-dependent transmit phase measurements. *Magn Reson Med*. 59:396-409
83. Nordmeyer-Massner JA, Wyss M, Andreisek G, Pruessmann KP, Hodler J (2011) In vitro and in vivo comparison of wrist MR imaging at 3.0 and 7.0 tesla using a gradient echo sequence and identical eight-channel coil array designs. *J Magn Reson Imaging*. 33:661-667
84. Ladd ME, Bachert P, Meyerspeer M, et al. (2018) Pros and cons of ultra-high-field MRI/MRS for human application. *Prog Nucl Magn Reson Spectrosc*. 109:1-50

85. Hansson B, Garzón B, Lövdén M, Björkman-Burtscher IM (2024) Decrease of 7T MR short-term effects with repeated exposure. *Neuroradiology*. 66:567-575
86. Cerezal L, Abascal F, García-Valtuille R, Del Piñal F (2005) Wrist MR arthrography: how, why, when. *Radiol Clin North Am*. 43:709-731
87. Omar NN, Mahmoud MK, Saleh WR, et al. (2019) MR arthrography versus conventional MRI and diagnostic arthroscope in patients with chronic wrist pain. *Eur J Radiol Open*. 6:265-274
88. Thomsen N, Besjakov J, Björkman A (2018) Accuracy of pre- and postcontrast, 3T indirect MR arthrography compared with wrist arthroscopy in the diagnosis of wrist ligament injuries. *J Wrist Surg*. 7:382-388
89. Pahwa S, Srivastava DN, Sharma R, Gamanagatti S, Kotwal PP, Sharma V (2014) Comparison of conventional MRI and MR arthrography in the evaluation wrist ligament tears: a preliminary experience. *Indian J Radiol Imaging*. 24:259-267
90. Dietrich TJ, Toms AP, Cerezal L, et al. (2021) Interdisciplinary consensus statements on imaging of scapholunate joint instability. *Eur Radiol*. 31:9446-9458
91. Lee RKL, Griffith JF, Ng AWH, Nung RCH, Yeung DKW (2016) Wrist traction during MR arthrography improves detection of triangular fibrocartilage complex and intrinsic ligament tears and visibility of articular cartilage. *Am J Roentgenol*. 206:155-161
92. Eladawi S, Balamoody S, Amerasekera S, Choudhary S (2022) 3T MRI of wrist ligaments and TFCC using true plane oblique 3D T2 Dual Echo Steady State (DESS) - A study of diagnostic accuracy. *Br J Radiol*. 95:20210019
93. Park HJ, Lee SY, Park NH, et al. (2016) Three-dimensional isotropic T2-weighted fast spin-echo (VISTA) ankle MRI versus two-dimensional fast spin-echo T2-weighted sequences for the evaluation of anterior talofibular ligament injury. *Clin Radiol*. 71:349-355
94. Nozaki T, Wu W Der, Kaneko Y, et al. (2017) High-resolution MRI of the ulnar and radial collateral ligaments of the wrist. *Acta radiol*. 58:1493-1499
95. Shahabpour M, De Maeseneer M, Pouders C, et al. (2011) MR imaging of normal extrinsic wrist ligaments using thin slices with clinical and surgical correlation. *Eur J Radiol*. 77:196-201
96. von Borstel D V., Wang M, Small K, Nozaki T, Yoshioka H (2017) High-resolution 3T MR imaging of the triangular fibrocartilage complex. *Magn Reson Med Sci*. 16:3-15
97. Ringler MD, Murthy NS (2015) MR Imaging of Wrist Ligaments. *Magn Reson Imaging Clin N Am*. 23:367-391
98. Mugler JP (2014) Optimized three-dimensional fast-spin-echo MRI. *J Magn Reson Imaging*. 39:745-767
99. Shahabpour M, Staelens B, Van Overstraeten L, et al. (2015) Advanced imaging of the scapholunate ligamentous complex. *Skeletal Radiol*. 44:1709-1725

100. Park HJ, Lee SY, Kang KA, et al. (2018) Comparison of two-dimensional fast spin echo T_2 weighted sequences and three-dimensional volume isotropic T_2 weighted fast spin echo (VISTA) MRI in the evaluation of triangular fibrocartilage of the wrist. *Br J Radiol.* 91:20170604
101. Jung JY, Yoon YC, Jung JY, Choe B-K (2013) Qualitative and quantitative assessment of wrist MRI at 3.0T: comparison between isotropic 3D turbo spin echo and isotropic 3D fast field echo and 2D turbo spin echo. *Acta Radiol*. 54:284-291
102. Kato H, Nakamura R, Shionoya K, Makino N, Imaeda T (2000) Does high-resolution MR imaging have better accuracy than standard MR imaging for evaluation of the triangular fibrocartilage complex? *J Hand Surg Am*. 25:487-491
103. De Smet L (2005) Magnetic resonance imaging for diagnosing lesions of the triangular fibrocartilage complex. *Acta Orthop Belg*. 71:396-398
104. Manton GL, Schweitzer ME, Weishaupt D, et al. (2001) Partial interosseous ligament tears of the wrist: difficulty in utilizing either primary or secondary MRI signs. *J Comput Assist Tomogr*. 25:671-676
105. Magee T (2009) Comparison of 3T MRI and arthroscopy of intrinsic wrist ligament and TFCC tears. *Am J Roentgenol*. 192:80-85
106. Blazar PE, Chan PSH, Kneeland JB, Leatherwood D, Bozentka DJ, Kowalchick R (2001) The effect of observer experience on magnetic resonance imaging interpretation and localization of triangular fibrocartilage complex lesions. *J Hand Surg Am*. 26:742-748
107. Morley J, Bidwell J, Bransby-Zachary M (2001) A comparison of the findings of wrist arthroscopy and magnetic resonance imaging in the investigation of wrist pain. *J Hand Surg Am*. 26:544-546
108. Anderson ML, Skinner JA, Felmlee JP, Berger RA, Amrami KK (2008) Diagnostic comparison of 1.5 Tesla and 3.0 Tesla preoperative MRI of the wrist in patients with ulnar-sided wrist pain. *J Hand Surg Am*. 33:1153-1159
109. Prosser R, Harvey L, LaStayo P, Hargreaves I, Scougall P, Herbert RD (2011) Provocative wrist tests and MRI are of limited diagnostic value for suspected wrist ligament injuries: a cross-sectional study. *J Physiother*. 57:247-253
110. Boer BC, Vestering M, van Raak SM, van Kooten EO, Huis In 't Veld R, Vochteloo AJH (2018) MR arthrography is slightly more accurate than conventional MRI in detecting TFCC lesions of the wrist. *Eur J Orthop Surg Traumatol.* 28:1549-1553
111. Greditzer HG, Zeidenberg J, Kam CC, et al. (2016) Optimal detection of scapholunate ligament tears with MRI. *Acta radiol*. 57:1508-1514
112. Van Dyck P, Zazulia K, Smekens C, Heusdens CHW, Janssens T, Sijbers J (2019) Assessment of anterior cruciate ligament graft maturity with conventional magnetic resonance imaging: a systematic literature review. *Orthop J Sport Med*. 7:2325967119849012
113. Grassi A, Bailey JR, Signorelli C, et al. (2016) Magnetic resonance imaging after anterior cruciate ligament reconstruction: a practical guide. *World J Orthop*. 7:638-649

114. Claes S, Verdonk P, Forsyth R, Bellemans J (2011) The “ligamentization” process in anterior cruciate ligament reconstruction: what happens to the human graft? A systematic review of the literature. *Am J Sports Med*. 39:2476-2483
115. Hooghof JT, de Vries AJ, Meys TWGM, Dening J, Brouwer RW, van Raay JJAM (2022) MRI signal intensity of anterior cruciate ligament graft after transtibial versus anteromedial portal technique (TRANSIG): a randomised controlled clinical trial. *Knee*. 39:143-152
116. Lutz PM, Achtnich A, Schütte V, Woertler K, Imhoff AB, Willinger L (2022) Anterior cruciate ligament autograft maturation on sequential postoperative MRI is not correlated with clinical outcome and anterior knee stability. *Knee Surgery, Sport Traumatol Arthrosc*. 30:3258-3267
117. Hakozaki A, Niki Y, Enomoto H, Toyama Y, Suda Y (2015) Clinical significance of T2*-weighted gradient-echo MRI to monitor graft maturation over one year after anatomic double-bundle anterior cruciate ligament reconstruction: a comparative study with proton density-weighted MRI. *Knee*. 22:4-10
118. Kiapour AM, Ecklund K, Murray MM, et al. (2019) Changes in cross-sectional area and signal intensity of healing anterior cruciate ligaments and grafts in the first 2 years after surgery. *Am J Sports Med*. 47:1831-1843
119. Panos JA, Devitt BM, Feller JA, Klemm HJ, Hewett TE, Webster KE (2021) Effect of time on MRI appearance of graft after ACL reconstruction: a comparison of autologous hamstring and quadriceps tendon grafts. *Orthop J Sport Med*. 9:23259671211023512
120. Putnis SE, Klasan A, Oshima T, et al. (2022) Magnetic resonance imaging assessment of hamstring graft healing and integration 1 and minimum 2 years after ACL reconstruction. *Am J Sports Med*. 50:2102-2110
121. Zhang Y, Liu S, Chen Q, Hu Y, Sun Y, Chen J (2020) Maturity progression of the entire anterior cruciate ligament graft of insertion-preserved hamstring tendons by 5 years: a prospective randomized controlled study based on magnetic resonance imaging evaluation. *Am J Sports Med*. 48:2970-2977
122. Micic I, Kholinne E, Kwak JM, Koh KH, Jeon IH (2019) Osteolysis is observed around both bioabsorbable and nonabsorbable anchors on serial magnetic resonance images of patients undergoing arthroscopic rotator cuff repair. *Acta Orthop Traumatol Turc*. 53:414-419
123. Tan S, Ghumman SS, Ladouceur M, Moser TP (2014) Carpal angles as measured on CT and MRI: can we simply translate radiographic measurements? *Skeletal Radiol*. 43:1721-1728
124. Tang JB, Giddins G (2016) Why and how to report surgeons’ levels of expertise. *J Hand Surg Eur Vol*. 41:365-366
125. Obuchowski NA (2004) How many observers are needed in clinical studies of medical imaging? *Am J Roentgenol*. 182:867-869
126. Heiss R, Weber MA, Balbach E, et al. (2023) Clinical application of ultrahigh-field-strength wrist MRI: a multireader 3T and 7T comparison study. *Radiology*. 307:1-8

127. Båth M, Hansson J (2016) VGC analyzer: a software for statistical analysis of fully crossed multiple-reader multiple-case visual grading characteristics studies. *Radiat Prot Dosimetry*. 169:46-53
128. Båth M (2010) Evaluating imaging systems: practical applications. *Radiat Prot Dosimetry*. 139:26-36
129. Efron B, Tibshirani R (1986) Bootstrap methods for standard errors, confidence intervals, and other measures of statistical accuracy. *Stat Sci*. 1:54-77
130. LaFleur BJ, Greevy RA (2009) Introduction to permutation and resampling-based hypothesis tests. *J Clin Child Adolesc Psychol*. 38:286-294
131. Kitis A, Celik E, Aslan UB, Zencir M (2009) DASH questionnaire for the analysis of musculoskeletal symptoms in industry workers: a validity and reliability study. *Appl Ergon*. 40:251-255
132. MacDermid JC (1996) Development of a scale for patient rating of wrist pain and disability. *J Hand Ther*. 9:178-183
133. Dewan AK, Chhabra AB, Khanna AJ, Anderson MW, Brunton LM (2013) Magnetic resonance imaging of the hand and wrist: techniques and spectrum of disease: AAOS exhibit selection. *J Bone Jt Surg*. 95:e68
134. Taljanovic MS, Goldberg MR, Sheppard JE, Lee F (2011) US of the intrinsic and extrinsic wrist ligaments and triangular fibrocartilage complex - normal anatomy and imaging technique. *Radiographics*. 31:e44
135. Taljanovic MS, Sheppard JE, Jones MD, Switlick DN, Hunter TB, Rogers LF (2008) Sonography and sonoarthrography of the scapholunate and lunotriquetral ligaments and triangular fibrocartilage disk: initial experience and correlation with arthrography and magnetic resonance arthrography. *J Ultrasound Med*. 27:179-191
136. Foster BH, Shaw CB, Boutin RD, et al. (2019) A principal component analysis-based framework for statistical modeling of bone displacement during wrist maneuvers. *J Biomech*. 85:173-181
137. Tian Y, Chaudhari AJ, Nayak KS (2025) Three dimensional real-time MRI for the comprehensive evaluation of wrist kinematics. *J Magn Reson Imaging*. 61:2648-2651
138. Zarenia M, Arpinar VE, Nencka AS, Muftuler LT, Koch KM (2022) Dynamic tracking of scaphoid, lunate, and capitate carpal bones using four-dimensional MRI. PLoS One. 17:e0269336
139. Imada AO, Eldredge J, Wells L, Moneim MS (2023) Review of surgical treatment for chronic scapholunate ligament reconstruction: a long-term study. *Eur J Orthop Surg Traumatol*. 33:787-793

Printed by Media-Tryck, Lund 2025 NORDIC SWAN ECOLABEL 3041 0903

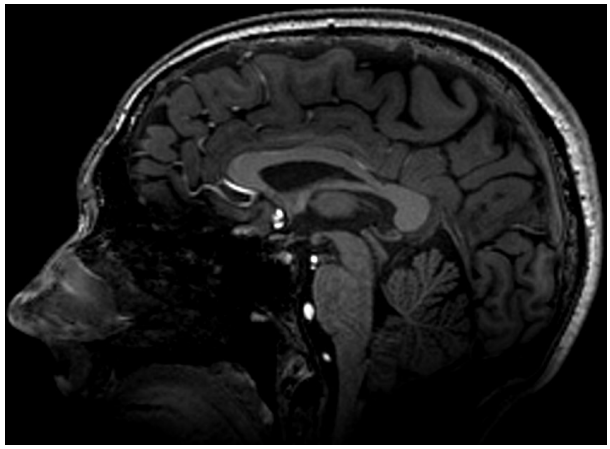

The author, Simon Götestrand

LUND UNIVERSITY

FACULTY OF MEDICINE

Diagnostic Radiology
Department of Clinical Sciences, Lund

Lund University, Faculty of Medicine
Doctoral Dissertation Series 2025:92
ISBN 978-91-8021-745-3
ISSN 1652-8220